



## Research paper

# Design and implementation of electric vehicle with autonomous motion and steering control system using single board computer and sensors

Zuber Basha Shaik, Samineni Peddakrishna

School of Electronics Engineering, VIT-AP University, Amaravati, Andhra Pradesh, 522241, India

## ARTICLE INFO

**Keywords:**

Electric vehicle  
Autonomous vehicle  
Autonomous electric vehicle  
Electronic control unit  
System on chip

## ABSTRACT

Autonomous motion and steering systems are crucial in electric vehicle (EV) technologies, enabling enhanced safety, efficiency, and user convenience. However, the integration of modern sensors and controllers and actuator mechanisms remains a significant challenge to achieving autonomous functionality in EVs. This study presents the design, integration, and implementation of an EV control system that operates in both manual and autonomous modes. In manual mode, the driver maintains complete control via the ignition key, emergency checks, and mechanisms for selecting direction and speed. Transitioning to autonomous mode involves integrating an autonomous vehicle electronic control unit (AV-ECU), which manages the existing electric vehicle electronic control unit (EV-ECU) as a subordinate unit. A Raspberry Pi 5 system-on-chip (SoC) serves as the master controller, coordinating motion and steering commands. In autonomous mode, the system leverages a range of sensors and actuators for navigation and control. The LIDAR-Lite v3HP sensor facilitates obstacle detection and distance measurement for real-time speed adjustments. A rotary encoder tracks steering angle and rotation direction, ensuring accurate maneuverability. Speed control is achieved through pulse width modulation (PWM) signals that adjust power to the motor, allowing for speeds varying from 0 to 40 km/h. Responsive steering control is provided by a worm gear motor system, managed by a motor driver that interfaces with the single-board computer. The system's effectiveness was validated in a controlled campus environment, where it successfully enabled basic autonomous transportation. The incorporation of advanced sensors, electronic control units, actuators, and real-time data collection demonstrated the practical application of autonomous driving technologies, emphasizing the system's safety, efficiency, and potential for implementation in real-world scenarios.

## 1. Introduction

The development and deployment of autonomous vehicles (AVs) have been significantly shaped by the groundbreaking achievements of Stanley and Boss, which have laid a foundation for advancements in this technology. Stanley's success in the 2005 DARPA Grand Challenge, which showcased the capabilities of self-driving vehicles in difficult desert environments, marked a pivotal moment in the evolution of AVs [1]. Building on this success, Boss further advanced the technology by tackling the challenges of navigating urban environments through the implementation of various sensors and a sophisticated planning system for decision making and navigation [2]. These early successes have generated a transformation in the automotive sector, pushing AVs toward a future full of possibilities and potential for growth. The initial focus of the development of AV was personal transportation, with companies such as Baidu and WeRide offering robotaxis in specific zones with

clear weather and light traffic conditions [3]. Researchers are making notable progress in the development of autonomous vehicles designed for various road traffic conditions, fueled by advancements in artificial intelligence (AI) and sensor technology. Recent advancements in path tracking utilizing nonlinear model predictive control (NMPC) enhance both accuracy and stability, thereby facilitating precise and reliable navigation for autonomous vehicles in urban and high-speed environments [4]. The successful development and deployment of autonomous electric vehicles (AEVs) requires considerable investments in research, infrastructure, and manufacturing. The associated costs of acquiring sensors, computing hardware, and software development can pose challenges to mass production and affordability [5]. Furthermore, the integration of autonomous systems into existing vehicles requires significant modifications and rigorous testing to ensure safety and reliability [6]. Enhanced battery management systems (BMSs) significantly improve energy storage efficiency, thermal management, and reliability, thereby

\* Corresponding author.

E-mail address: [krishna.samineni@gmail.com](mailto:krishna.samineni@gmail.com) (S. Peddakrishna).

contributing to the sustainability of advanced EVs [7][8]. Overcoming these challenges is essential for fully realizing the potential of AEVs and facilitating their widespread adoption. One promising strategy for addressing these issues involves retrofitting current EVs into AEVs. This approach leverages the existing infrastructure and components within EVs, such as electric motors, batteries, and onboard computing systems, to incorporate autonomous driving capabilities. Advancements in permanent magnet synchronous Motors (PMSMs) and switched reluctance motors (SRMs) enhance energy efficiency and minimize environmental impact, facilitating the retrofitting of Advanced EVs [8].

Using these existing elements, developers can potentially reduce the overall costs associated with the deployment of AEVs, enhancing the accessibility of autonomous driving technology to a broader market [9]. The conversion process begins with an assessment of the vehicle's mechanical components, which are critical to its drivetrain and chassis. EVs typically feature robust drivetrains designed to handle the torque requirements of electric motors. These drivetrains incorporate essential components, including axles, differentials, and suspension systems, establishing a solid foundation for the integration of autonomous features. In many instances, existing electric motors may be retained, and an electronic control unit (ECU) can be integrated to facilitate precise control over motor speed and torque, thereby enabling autonomous functionality [10]. This level of precise control is essential for the autonomous system to effectively execute maneuvers and maintain consistent vehicle stability [11]. The retrofitting process encompasses not only the mechanical components but also the installation of various components and computing systems within the vehicle. These components, such as LIDAR, proximity sensors, rotary sensors, and relay systems, supply the autonomous system with real-time data essential for vehicle operation. This data is analyzed by a controller to identify obstacles and enable informed decision-making [12]. Furthermore, the battery pack in an EV serves as an essential resource during the conversion process, supplying power not only to the electric motor but also to the additional components required for autonomous driving [13]. Following the assessment of the existing components, the conversion process requires comprehensive software development and integration. Advanced software is crucial for managing the various elements of an autonomous driving system, including the installation of components responsible for controlling direction, speed, object distance measurement, and other vital functions [14].

These components collaborate to create a real-time AEV that can detect objects and navigate safely in relation to nearby obstacles. In addition, the integration of AEVs has the potential to transform public transportation and logistics. The following lists the contributions made by this work to the design and implementation of an AEV system that is suited for particular operational requirements, such as campus settings.

- The AEV is developed through the assembly and integration of essential components that facilitate manual driver control. The operator can manage the vehicle's functions using components such as the throttle, brake, and ignition system, with support from the ECU.
- Subsequently, the vehicle is equipped with a motion control and steering control system to facilitate autonomous operation. This process involves the integration of essential hardware components and the development of software to enable autonomous vehicle control.
- The vehicle is tested in a designated open area to validate its autonomous capabilities. The testing focuses on verifying the speed control, steering precision, obstacle detection, and safe navigation of the system, demonstrating the effectiveness of integrated hardware and software for real-world use.
- The LIDAR-Lite v3HP sensor ensures reliable obstacle detection, accurately detecting objects up to 40 meters with  $\pm 2.5$  cm precision. The system dynamically adjusts speed based on object proximity,

ranging from 8 km/h for objects over 15 meters to a complete halt for objects within 5 meters.

- Steering precision and safety are achieved through the integration of a Raspberry Pi, rotary encoder, and PWM-driven worm motor, with a 1:22.5 steering ratio and a 35° safety angle threshold. Additional features include proximity sensors for steering adjustments and an emergency stop switch that immediately halts the vehicle during emergencies, ensuring reliable and safe autonomous operation.

The following sections will provide a thorough literature review, outlining the essential components and methodologies utilized in the development of autonomous vehicles.

## 2. Related work

In recent times, increasing fossil fuel costs and growing environmental concern have led to a renewed focus on EVs in the automotive industry. Unlike traditional vehicles that rely on internal combustion engines (ICE) as the main source of propulsion and fuel tanks for storage, EVs primarily use batteries, controllers, and electric motors for propulsion [15]. While, it is important to note that EVs are not solely battery-powered, as they can be categorized into two main types, which are pure electric vehicles and hybrid electric vehicles (HEVs). Pure electric vehicles operate solely on electric propulsion systems, with batteries being the main energy source. Whereas HEVs combine electric motors with another power source, typically integrating an internal combustion engine with batteries [16]. HEVs, like the Toyota Prius, employ a combination of an ICE and an electric motor to enhance fuel efficiency and reduce emissions. This advanced dual-powertrain system allows HEVs to efficiently switch between or utilize both power sources simultaneously, thereby optimizing overall performance and fuel economy based on varying driving conditions [17]. The ability to adapt power utilization is a key advantage of HEVs. This feature not only extends driving ranges compared to plug-in electric vehicles (PEVs), but also retains the environmental benefits associated with electric propulsion.

In contrast, the main reason behind the transition to PEVs is the environmental necessity. Research conducted by esteemed organizations has demonstrated that the transportation sector is a substantial contributor to greenhouse gas emissions, significantly affecting global CO<sub>2</sub> levels [18]. PEVs offer the significant benefit of producing zero tailpipe emissions, which substantially diminishes their environmental footprint compared to HEVs, which still depend on gasoline for part of their energy needs. In addition to their lower emissions, PEVs contribute positively to air quality. Studies suggest that the widespread adoption of PEVs could result in improved air quality in urban settings, thereby decreasing public health concerns related to air pollution [19]. Economic considerations are increasingly influencing the growing interest in PEVs. Concerns regarding fluctuating oil prices and energy security have led to a movement towards alternative fuel sources. PEVs offer a degree of independence from unstable oil markets, which may lead to more predictable fuel expenses for consumers. Additionally, improvements in battery technology are gradually lowering production costs for PEVs, enhancing their economic competitiveness relative to HEVs [20]. EVs, such as the Tesla models, function entirely on electric energy accumulated in batteries for propulsion. These vehicles generate no tailpipe emissions and can be powered by renewable energy sources, positioning them as a more environmentally sustainable mode of transportation [21].

The transition to PEVs marks a substantial move towards more sustainable transportation. This shift entails several implementation challenges that must be addressed. A primary concern is the driving range of batteries, as drivers often fear depleting power before reaching a charging station. Research conducted by [22] examines this issue, highlighting the necessity for improved battery range and an expanded charging infrastructure to mitigate driver concerns. The accessibility of charging

infrastructure is also critical. Research conducted by [23] emphasizes the significance of having a strong and readily accessible network of charging stations, especially in urban environments and along key travel corridors. Additionally, research conducted by [24] emphasizes the importance of advancing fast charging technologies to minimize charging durations and mitigate range anxiety. Several strategies for implementation, including advancements in battery technology, enhancements to energy management systems, and the expansion of charging infrastructure, have been evaluated to significantly improve the performance and range of PEVs [25].

This existing expertise and infrastructure developed for PEVs, serve as a solid foundation for the progress of AV technology. The rapid progression in AEV technology has led to the incorporation of sophisticated motion control and steering control systems to improve vehicle performance and safety. The use of controllers, combined with a range of sensors, actuators, electric motors, and advanced control algorithms, play a crucial role in this domain. The incorporation of these technologies involves complex systems that rely heavily on controllers to manage and coordinate the various components required for autonomous driving capabilities. This approach is validated through successful experiments that prove the concept. Building upon this concept, another study aimed to create entirely new autonomous vehicles [26]. These vehicles excel at following a route that has been previously driven by a human. To navigate and detect obstacles effectively, they rely on a comprehensive suite of sensors, including GPS (global positioning system), gyroscopes, accelerometers, and light sensors. This approach holds promise for controlled environments or repetitive tasks. To achieve this, controllers play a pivotal role in these systems by managing data from various sensors and implementing control algorithms to facilitate autonomous driving. Morales et al. present a thorough survey of path planning techniques for autonomous vehicles, underscoring the essential function of controllers in overseeing these complex tasks [27].

Research studies have explored the advancement of autonomous vehicles capable of navigating predetermined routes utilizing a range of sensors [28]. The integration of sensors with actuators is essential for effective vehicle motion control. This process entails collecting data from various sensors and subsequently activating vehicle components to achieve specific functionalities. Single-board computers (SBCs) are particularly advantageous in this domain due to their compact size, processing capabilities, and cost efficiency. A wide array of studies have illustrated the successful integration of sensors, including GPS, gyroscopes, accelerometers, and LIDAR, with SBCs [29]. Pannu et al. notably demonstrated the feasibility of utilizing a Raspberry Pi as the central control unit for a prototype of an autonomous vehicle [30]. The design featured a range of sensors, including ultrasonic sensors for obstacle detection and a camera for lane tracking. The Raspberry Pi effectively processed the sensor data and managed the vehicle's movements, demonstrating the capabilities of SBCs in autonomous vehicle applications. Additionally, Mohammed et al. presented a cost-effective solution utilizing a single camera along with CNN-based steering prediction, which facilitates the efficient transformation of conventional vehicles into autonomous systems [31]. Budisteanu et al. explored the use of AI techniques on low-cost platforms for the development of self-driving cars, emphasizing the role of SBCs in facilitating intelligent decision-making [32]. Ollukaren and McFall further highlighted the cost-effectiveness of small robotic systems in their research on a low-cost autonomous ground vehicle platform, demonstrating the accessibility of this technology for research and development purposes [33]. Wall et al. illustrated the application of economical components such as ultrasonic sensors, GPS modules, and microcontrollers in the development of cost-effective autonomous vehicles that can navigate routes and avoid obstacles [34].

In recent times, there has been a shift towards the integration of advanced sensors, such as LIDAR, to enhance perception capabilities. Cui et al. examined the application of roadside LIDAR data for vehicle tracking in connected vehicle systems, emphasizing the potential of LIDAR to improve situational awareness [35]. Yoshioka et al. conducted a

study that showcased the efficacy of LIDAR technology in real-time object classification for autonomous vehicles, highlighting its capability to differentiate among various types of obstacles and road users [36]. Becsi et al. advanced low-cost 3D LIDAR technology by integrating it with SLAM systems, resulting in improved precision in environmental mapping and navigation for experimental vehicle [37]. Building upon this foundational research, Jason Valera and colleagues developed a system that enables navigation along a predetermined route while efficiently avoiding obstacles. The vehicle accomplishes this by integrating data from multiple sensors, including a 3D scanning LIDAR, a camera, and GPS technology [38]. Furthermore, it utilizes a Beaglebone SBC to handle motor driver signals and process data from the sensors. El-Hassan et al. also conducted a thorough experimental study on the integration of various sensors, including LIDAR, within a low-cost autonomous vehicle prototype, highlighting the significance of sensor fusion for enhanced perception and control [39]. These studies collectively emphasize the promise of integrating SBCs with various sensors, including LIDAR, to facilitate affordable and effective autonomous vehicle navigation. Isik and Çetin developed a multifunctional and cost-efficient autonomous mobile robot (AMR), highlighting the versatility of such platforms for diverse applications. In addition to this, Faisal et al. demonstrated the application of YOLO-based object detection combined with distance measurement, enhancing real-time obstacle detection and improving vehicle safety mechanisms [40]. Furthermore, Saputro et al. investigated the application of proportional-integral-derivative (PID) control in adaptive cruise control systems for EV prototypes, emphasizing the importance of maintaining safe following distances. Recent research has focused on the advancement of adaptive and intelligent control systems for AVs [41]. Isik and Çetin developed a multifunctional and cost-efficient AMR, highlighting the versatility of such platforms for various applications. Additionally, Mariaraja et al. contributed to the field by designing and implementing an advanced automatic driving system based on a Raspberry Pi, which includes functionalities such as lane detection, obstacle avoidance, and traffic sign recognition [42].

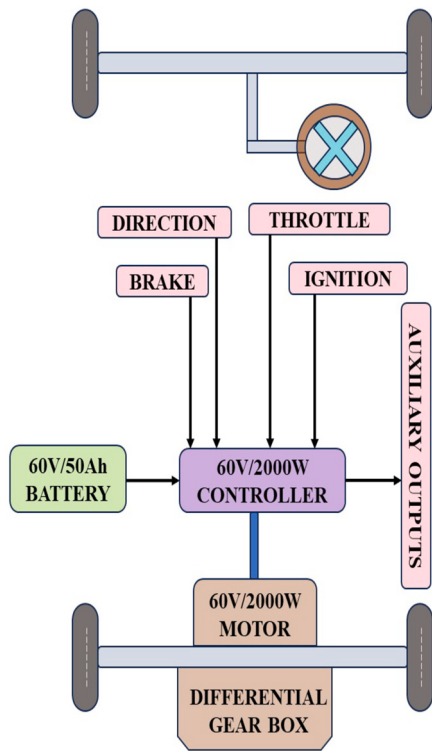
In addition to basic autonomous navigation methods, Lavanya et al. focused on developing adaptive throttle and brake control systems for cruise control specifically tailored for vehicles accommodating individuals with disabilities, thereby highlighting the potential for improving accessibility and driving assistance [43]. Furthermore, Saputro et al. explored the application of PID control for adaptive cruise control (ACC) in EV prototypes, considering the importance of maintaining safe following distances [44]. Furthermore, efforts have been made to incorporate intelligent speed control into AEVs. Setyawan and Happyanto emphasized the importance of adaptive algorithms to enhance both energy efficiency and performance in this context [45]. They demonstrated the implementation of such systems, utilizing sensor data and environmental information to optimize speed and energy consumption. Additionally, Shinde et al. examined the integration of LIDAR technology with vehicle-to-vehicle communication to improve ACC performance [46]. Their findings highlight the potential of advanced sensors to enhance safety and traffic flow.

To further contextualize these advancements, Table 1 provides a detailed comparison of the proposed system with related works in the literature. This comparison highlights key innovations, mode of operation, speed and motion control strategies, steering mechanisms, and the power management achieved by various systems. Notably, while earlier works have focused on features such as collision prevention, obstacle navigation, or ACC, many lack hardware-specific mechanisms or demonstrate limited improvements in energy efficiency. These studies collectively illustrate a clear progression from fundamental autonomous platforms to more advanced systems. However, challenges persist in achieving robust perception, reliable decision-making, and ensuring the safety of autonomous vehicles in real-world environments. This study aims to build upon this foundation by focusing on the practical implementation of an AEV with manual driver control capabilities, which will be further enhanced with motion and steering control systems for au-

**Table 1**

Comparison of the Proposed Work with Related Works Based on Power Management.

Ref	Key Innovation	Mode of Operation	Speed and Motion Control	Steering Mechanism	Power Management Over Conventional Systems
[29]	Obstacle detection and collision prevention	Autonomous	Dynamically managed	Lacks hardware-specific mechanisms	Limited improvement
[30]	Autonomous navigation	Dual mode	No adaptive cruise control	Lacks hardware-specific mechanisms	Minimal improvement
[33]	Object tracking	Manual	No adaptive cruise control	Steering controlled manually	Slight improvement
[34]	Obstacle avoidance and navigation	Dual mode	Speed control with GPS	Lacks hardware-specific mechanisms	Marginal improvement
[38]	Obstacle avoidance and navigation	Autonomous	No adaptive cruise control	Steering mechanism not mentioned	Marginal improvement
[42]	Obstacle detection and navigation	Autonomous	Lacks motion control	Adjustments via motor drivers	Limited improvement
[43]	Obstacle avoidance	Autonomous	No adaptive mechanisms	Not explicitly discussed	Moderate improvement
[44]	Speed and distance control	Autonomous	Adaptive cruise control	Focus on speed and distance control	Moderate improvement
[45]	Intelligent speed control	Dual mode	No adaptive mechanisms	No specific steering mechanism	Marginal improvement
[46]	V2V communication	Semi-autonomous	Adaptive cruise control	Not emphasized	Limited improvement
Present Work	Lidar-based detection, speed, and steering control	Dual modes	PWM-based speed and adaptive cruise control	Worm gear-based hardware-specific	15-20% improvement in driving range due to regenerative braking

**Fig. 1.** Block Diagram of a General Electric Vehicle for Present Work.

tonomous operation. The decision to conduct testing in an open area aligns with the practical focus observed in recent research, thereby contributing to the expanding body of knowledge in the development of real-world AVs.

### 3. Design methodology

#### 3.1. EV design methodology and working principle (manual mode)

The Fig. 1 shows the block diagram depicts the key components and their connections used for implementation of the present work and proof of concept of the real time EV.

##### 3.1.1. Electronic control unit in an electric vehicle

In the fast-paced world of EVs, the ECU plays a critical role in managing and coordinating various components to ensure optimal vehicle

performance. One of the critical parts of this system is the 60 V/2000 W controller, which plays a crucial role in managing the power flow from the battery to the motor, processing various signals from the driver, and ensuring the overall functionality of the vehicle. Fig. 2 illustrates a typical setup involving a high-performance L5 BLDC controller device, 60 V/2000 W brushless DC (BLDC) motor, a 60 V/50Ah LiFePO4 battery, a miniature circuit breaker (MCB), Hall sensors, and multiple control signals. The 60 V/2000 W controller typically operates at a nominal voltage of 60 volts and has a power rating of 2000 watts (60 V/2000 W), as specified. This controller is well-suited for our application, which demands substantial torque and speed. A detailed functional description of each component will be provided in the following subsections.

##### 3.1.2. Battery and power management

The battery in an EV is an advanced unit equipped with a BMS that is specifically designed to enhance performance and ensure safety. It is a 60 V/50Ah LiFePO4 (Lithium Iron Phosphate) battery with a storage capacity of 3000 watt-hours (Wh). However, the operating voltage we used in our work is 62.2 V, which is approximately 60 V, as indicated in the BMS application. The LiFePO4 battery is preferred for its exceptional thermal and chemical stability, extended cycle life, and built-in safety features when compared to other lithium-ion batteries. The BMS plays a key role by monitoring various parameters, including the battery's state of charge (SOC), state of health (SOH), and cell balancing. This oversight helps prevent overcharging and deep discharging, ensuring long-term reliability. It also tracks temperature, voltage, and current to maintain safe operation. If any irregularities in the event occur, the BMS is capable of disconnecting the battery from the system to mitigate potential risks. Furthermore, the system balances charge levels across individual cells, promoting equitable usage and prolonging the battery's lifespan. Users can conveniently check the battery status via a mobile application connected to the BMS through Bluetooth. A sample representation of the battery's status is illustrated in Fig. 3, the BMS continuously monitors the voltage of each cell in real-time, prioritizing the balancing of any cell that exhibits significant deviation to ensure uniform voltage across the entire pack. This dynamic process shifts focus among different cells as needed, depending on their individual states during charging, discharging, or resting. When a cell approaches the balancing threshold, it is highlighted in red to indicate a minor voltage deviation and is then adjusted accordingly through continuous monitoring.

The battery is engineered to withstand harsh environmental conditions, featuring with an operating temperature range of -20 °C to +60 °C for discharge and 0 °C to +45 °C for charging, along with an IP65 or higher protection rating for dust and water resistance. Furthermore, a MCB is installed between the battery and the ECU to safeguard the electrical circuit from potential damage caused by overloads or short

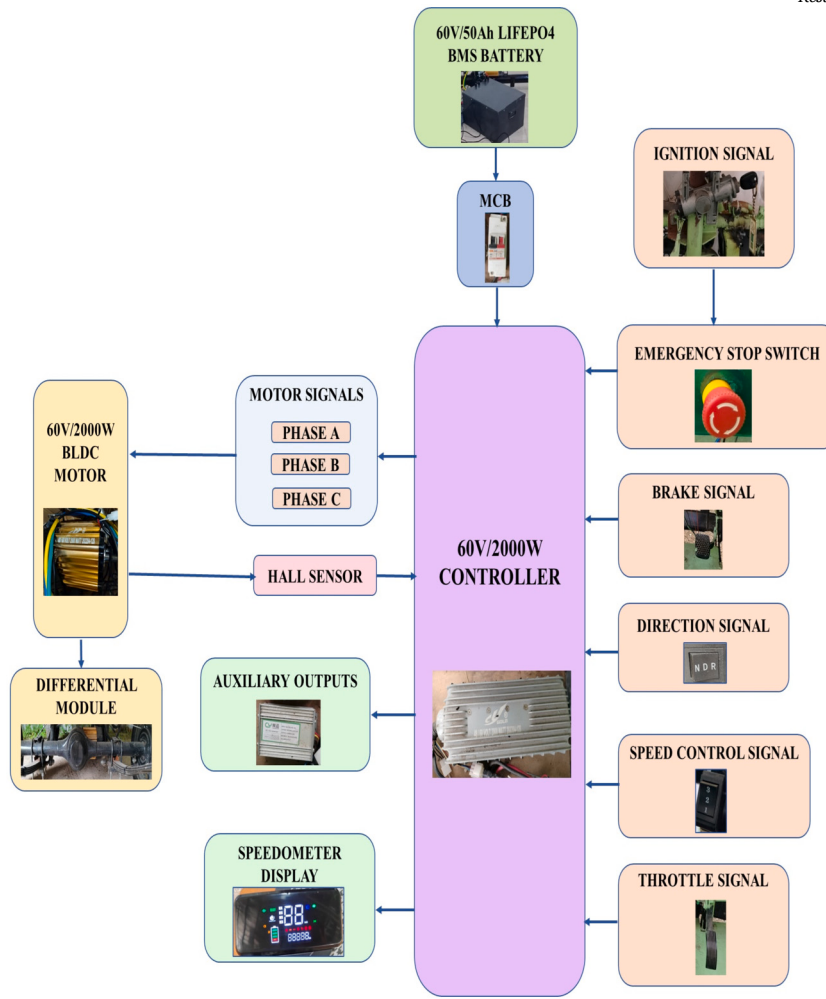


**Fig. 2.** Block Diagram of EV-ECU.

circuits. The MCB functions to automatically interrupt the flow of excessive current, thereby preventing overheating and reducing the risk of fires, which in turn enhances the safety and reliability of the electric vehicle. Additionally, the MCB can be manually reset, facilitating a swift recovery once the issue has been addressed.

### 3.1.3. DC motors and differential

For the implementation the selected 60 V/2000 W BLDC motor, a set of specifications is typically provided that outlines its performance and operational characteristics. One significant feature is regenerative braking, which enables the motor to recover energy during deceleration, thereby enhancing overall efficiency and prolonging battery life. Additionally, the motor is equipped with built-in protection mechanisms against overcurrent and overheating, ensuring safe operation even under substantial loads. The brushless design also minimizes operational noise, making it suitable for environments where noise sensitivity is a concern. Moreover, the motor generally possesses a robust IP54 protection rating, which ensures resistance against dust and water ingress, making it ideal for various environmental conditions. These attributes contribute to making the 60 V/2000 W BLDC motor a reliable and efficient option for high-performance applications. In conjunction with the motor, differentials play an essential role in vehicles equipped with multiple drive wheels. They enable wheels on the same axle to rotate at differing speeds during turns, facilitating smoother cornering, reducing tire wear, and enhancing overall handling. Differentials are crucial for the efficient distribution of power from the BLDC motor to the rear wheels, ensuring they operate at appropriate speeds during turns. The differen-

tial utilized in this context features electronic controls that adjust the torque delivered to each wheel. This capability not only enhances handling performance but also provides valuable safety features, including traction control and stability management.

### 3.1.4. Motor controller and its input control signals

Motor control is a fundamental function of the ECU, which involves the accurate generation of three-phase signals (Phase A, Phase B, and Phase C) to operate the BLDC motor. Unlike traditional brushed motors, the BLDC motor employs electronic commutation, eliminating the need for physical brushes and commutators. This absence of brushes not only reduces maintenance requirements but also extends the motor's lifespan, making it an optimal choice for electric vehicles. The chosen motor, rated at 60 V/2000 W, is a robust and powerful solution capable of delivering significant torque and speed. The controller effectively regulates the power flow from the battery to the motor, ensuring that the motor receives the appropriate amount of power based on the driver control inputs.

Additionally, the auxiliary output of the 60 V/2000 W motor controller offers a reliable power supply for external devices and accessories as a notable feature. This output typically provides either 5 V or 12 V DC, allowing for the operation of various peripheral devices, including sensors, indicators, and small control mechanisms. This functionality facilitates the seamless integration of these components into the overall system, thereby obviating the need for separate power supplies and streamlining wiring complexity while minimizing potential points of failure. Moreover, the incorporation of auxiliary devices through the



Fig. 3. Battery Status Monitoring using BMS Application.

motor controller's auxiliary output enables centralized control and monitoring. This is particularly beneficial for integrating multiple control signals, such as ignition, throttle, brake, direction, and speed control signals, as illustrated in Fig. 2. Each of these signals requires a specific operating voltage input, and the controller manages them to effectively regulate the motor and other vehicle systems.

The ignition signal plays a fundamental role in initiating the vehicle's operation by energizing the ECU. It serves as the command signal that activates the ECU and other essential systems, ensuring they are properly initialized and prepared for use. Furthermore, it functions as a safety measure, preventing inadvertent starts or operation without the driver's explicit intention. Once the ECU is powered on, the throttle signal, which serves as the electrical equivalent of an accelerator pedal, communicates the driver's intended acceleration level to the controller. The controller evaluates this signal via three connections: positive, negative, and a signal connection, to make accurate adjustments to the motor's power output. This level of control over the motor's power is further refined by feedback from Hall sensors integrated within the BLDC motor. These sensors are essential for determining the precise position of the rotor, enabling the controller to synchronize phase signals with the rotor's position and ensuring efficient and smooth motor performance. The feedback system is based on Hall sensors A, B, and C, which are spaced 120 electrical degrees apart and connected to the controller. The controller analyzes these signals to establish the accurate timing for switching the motor phases. Subsequently, it generates pulse width modulation (PWM) signals with the appropriate duty cycles to regulate the voltage supplied to the motor windings, thereby managing the motor's speed and torque effectively. The Hall sensors continuously provide positional updates as the rotor spins, allowing the controller to

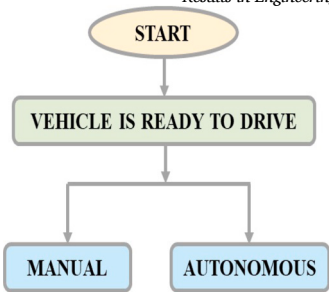


Fig. 4. Operating Driving Modes of Vehicle.

dynamically adjust the PWM duty cycles to meet the desired operating conditions.

Conversely, the break signal enables the user to decelerate or stop the motor. It typically involves a single connection that communicates with the controller to reduce or cut off power to the motor. The other control signal such as direction signal, generated by a switch in the driver's control panel, instructs the controller whether the vehicle should move forward or reverse. The controller then adjusts the phase sequence of the motor control signals to align with the intended direction of motion. This typically involves two connections that interact with the controller to switch between forward and reverse modes. Based on the direction, the speed mode signal allows the user to select different operational speed settings for the vehicle. This is achieved through three connections that interact with the controller. The controller is designed to monitor and adjust the motor's power output in order to maintain the desired speed under various conditions. It offers three pre-set operating modes to choose from - Eco Mode (Mode 0), Standard Mode (Mode 1), and Performance Mode (Mode 2). The speed control mode switch allows to switch between these modes. This mode selection is typically based on the need between performance and efficiency requirement. Mode 0 prioritizes energy efficiency by decreasing the motor's power output. Mode 1 offers a balance between performance and efficiency, providing moderate power output suitable for everyday use. Mode 2 delivers maximum power output, resulting in the highest achievable speed. To monitor the speed of a vehicle, a speedometer is used to display the current speed.

### 3.1.5. Working principle

The working principle of an electric vehicle involves a sequence of checks and initializations, starting with the driving mode selection, allowing the driver to choose between manual and autonomous driving modes.

In the proposed system, the driving mode is selected through a manual ignition key and an integrated switching mechanism, allowing smooth toggling between manual and autonomous modes. In manual mode, the driver retains full control of the vehicle using traditional inputs, including the ignition key, throttle, brake, and steering. This mode is particularly useful in scenarios requiring human intervention, such as during emergencies, initial operations, or environments unsuitable for autonomous navigation. In contrast, autonomous mode is activated via an electronic toggle or switch, which integrates the AV-ECU with the EV-ECU. Once activated, the system relies on data from sensors such as LIDAR and rotary encoders, coupled with pre-programmed control algorithms, to enable obstacle detection and adaptive speed control. This mode is designed for structured environments like campuses or controlled test zones, where autonomous functionality can be fully utilized. To further clarify the transition between the two modes, a Driving Mode Selector block has been added to Fig. 4. This component visually illustrates the connection between the two modes: manual mode, linked directly to driver inputs, and autonomous mode, driven by sensor inputs and managed by the AV-ECU. This dual-mode system provides flexibility and safety, addressing diverse operational needs while ensuring reliable performance in real-world applications. In manual mode, the driver is having full control over the vehicle including the activation of

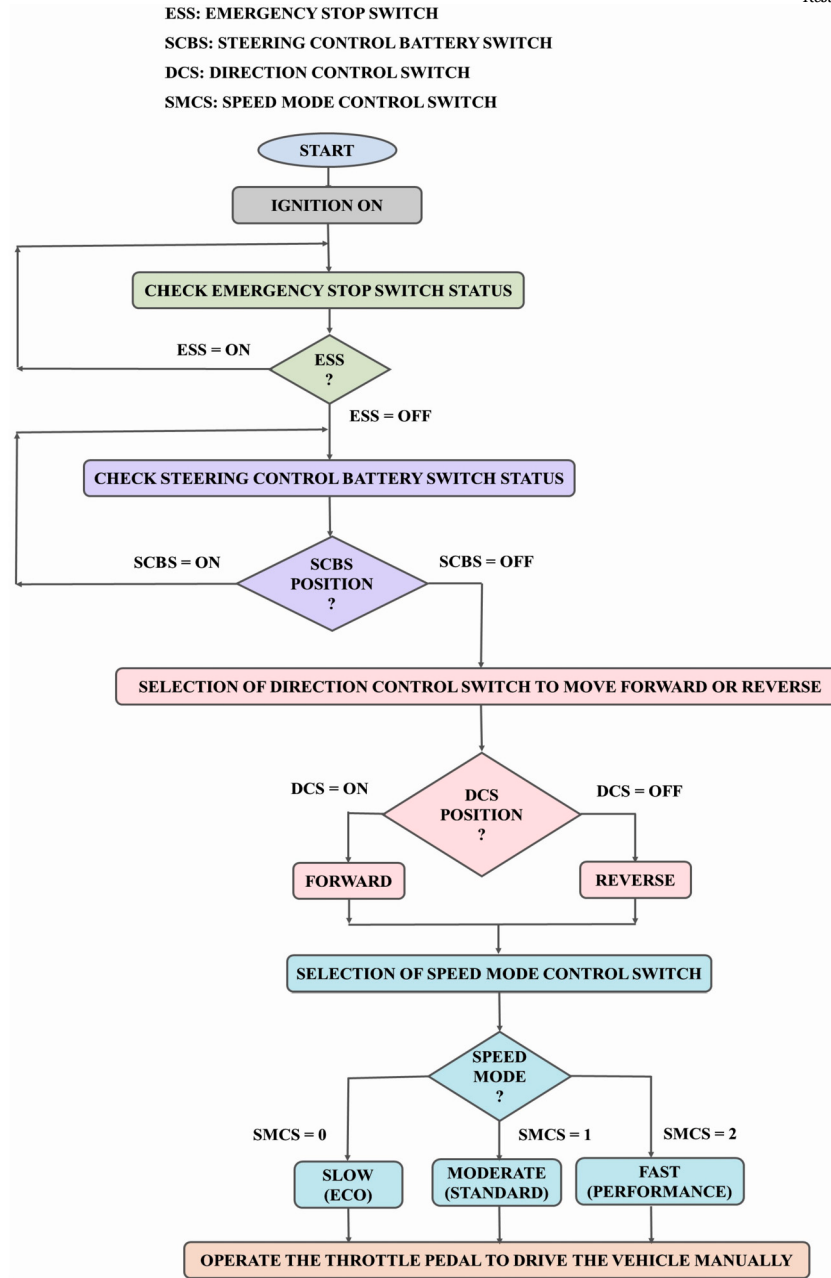


Fig. 5. Manual Driving Mode Operational Flowchart of Vehicle.

the ECU from ignition key, managing acceleration, braking, and steering. The manual mode operating procedure of the flow chart is presented in Fig. 5. Once, the ignition key is activated in the vehicle, the driver verifies the additional protection switches such as emergency stop switch status followed by steering control battery switch. These two switches need to be set in the OFF position to power up the vehicle and smooth rotation of the steering respectively. After the completion of these checks, the ECU is proceeding with the power-up sequence. Then, the driver selects the desired direction and speed using the direction control and speed mode selector.

The operational direction control mode manages the vehicle's movement between forward and reverse directions by manipulating the drive (D) and reverse (R) circuit pins within the designated electrical paths. When the two pins are in a short circuit position, the vehicle moves forward, while an open circuit position causes the vehicle to move in reverse.

Table 2  
Speed Mode Switch Selection Pins.

MODE	PIN-1 (Pink)	PIN-2 (Blue)	PIN-3 (Yellow)
MODE 0 (SLOW)	Short Circuited		Open Circuited
MODE 1 (MODERATE)	Open Circuited		
MODE 2 (FAST)	Open Circuited	Short Circuited	

The operational speed control mode in vehicle is slow (20 Kmph), moderate (33 Kmph) and fast (40 Kmph). The Mode 0, Mode 1 and Mode 2 of selecting speed mode involves short-circuit or open-circuit of the designated pins as shown in Table 2.

The signal output of the throttle sensor will be varied by pressing and releasing the throttle pedal.

Finally, the driver is manually slowing down or stopping the vehicle by pressing the brake pedal. The proof of concept of electric vehicle depicted in Fig. 6.



**Fig. 6.** Proof of Concept of Real Time EV.

The Fig. 7 shows the electric vehicle ECU part and wirings that describes the functions of the controller and other components that are used to operate the electric vehicle manually.

In autonomous mode, the advanced driver assistance system is taking control, using sensors and actuators to operate the vehicle with minimal driver intervention.

### 3.2. Methodology for motion control and steering control (autonomous)

The design methodology for developing a motion control and steering control system of an autonomous vehicle involves the hardware implementation and programming different components for controlling. The use of actuators, sensors and control unit covers the part of

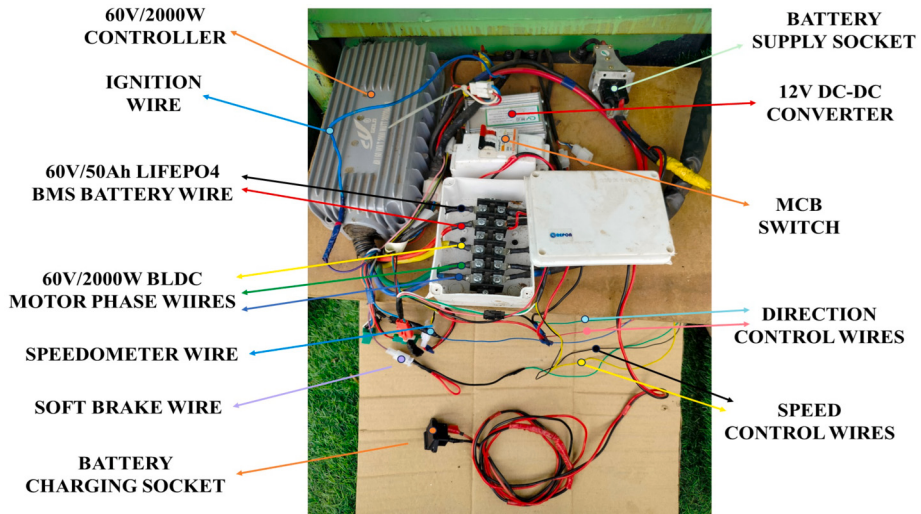


**Fig. 7.** Electric Vehicle ECU Part.

hardware design. Controlling of motion, steering, and safety mechanisms through programming covers the software design. Assembling the hardware components and programming on single-board computers combinedly covers the implementation of motion and steering control for autonomous driving. The combined block diagram of motion and steering control was depicted in Fig. 8. In order to achieve this, the development process for motion control and steering control are implemented separately as given in the following subsections and combined together.

#### 3.2.1. Motion control

In order to achieve autonomous operation, it is crucial to have the capability for motion control to enable obstacle avoidance and adaptive cruise control. This entails incorporating sensors that consistently collect data on the vehicle's environment, which is then analyzed and processed to make immediate adjustments to the vehicle's speed and direction. This process involves the integration of various sensors and actuators with a single board computer, as depicted in Fig. 9. A single board computer serves as the central control unit, responsible for overall control and processing of sensor and actuator data. One of the sensors used is the LIDAR-Lite v3HP, capable of measuring distances of an object up to 40 meters with an accuracy of  $\pm 2.5$  cm. This sensor sends object distance data to the controller for processing and takes the appropriate actions such as acceleration, deceleration, or stopping the vehicle using pulse width modulation control signal.

The process entails utilizing a PWM signal shown in Fig. 10 to regulate the vehicle's speed based on the distance from a detected object by continuously monitoring sensor information, as depicted in the flow diagram in Fig. 11. If the object is more than 15 meters away, the PWM control signal will operate with a 45% duty cycle, moving the vehicle at around 8 Km/h. If the object is in between 10-15 meters or equal to 15 meters away, the PWM control signal will operate with a 40% duty cycle, moving the vehicle at around 5 Km/h. If the object is between 5-10 or equal to 10 meters away, the vehicle will operate at 2 Km/h with a 35% duty cycle of PWM signal. And if the distance is less than 6 meters, the PWM signal will be adjusted to a 0% duty cycle to stop the vehicle immediately. For last two conditions both back left and right signal lights will turn ON and blow the horn.

The graph between PWM vs VARPP, VAECUSP and SPEED is shown in Fig. 12 gives the correlation between the PWM duty cycle and the corresponding voltages measured across a Raspberry Pi PWM pin (VARPP), the voltage across the ECU speedometer (VAECUSP), and the resultant speed. The data indicates that as the PWM signal increases, both voltages and speed undergo notable changes. Specifically, at VARPP, the

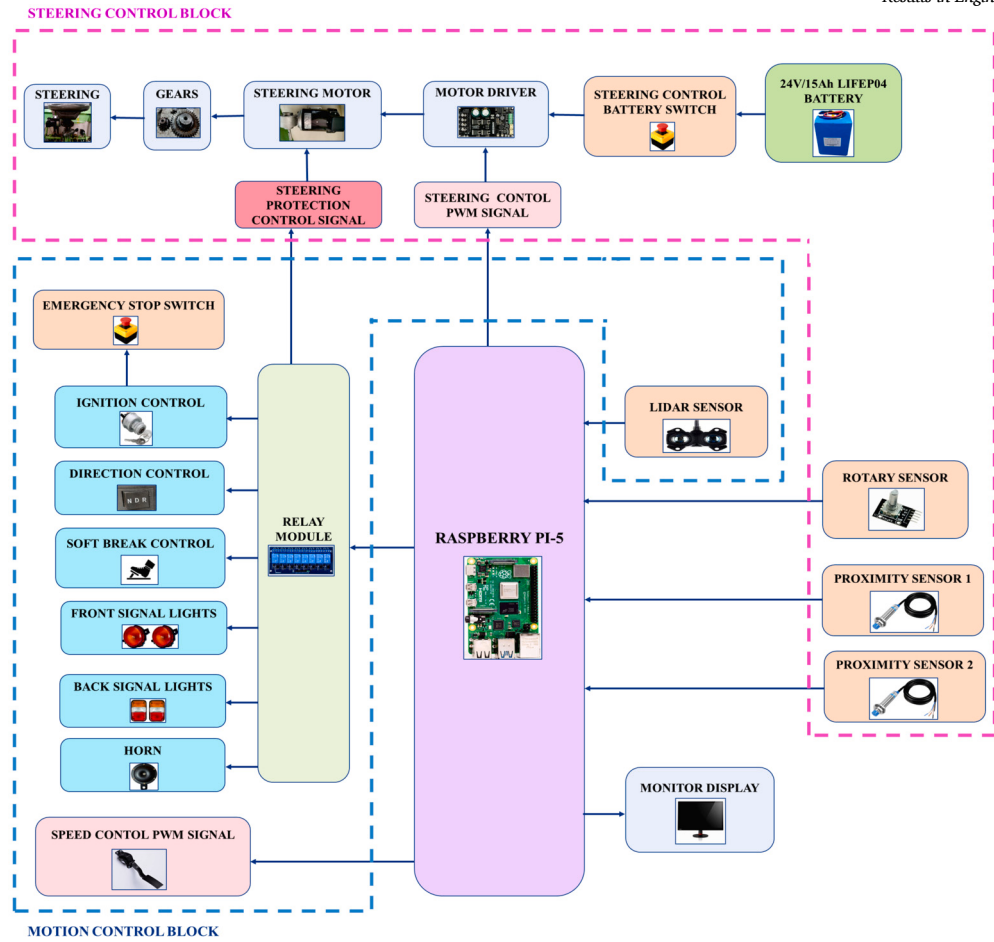


Fig. 8. Combined Block Diagram of Motion and Steering Control.

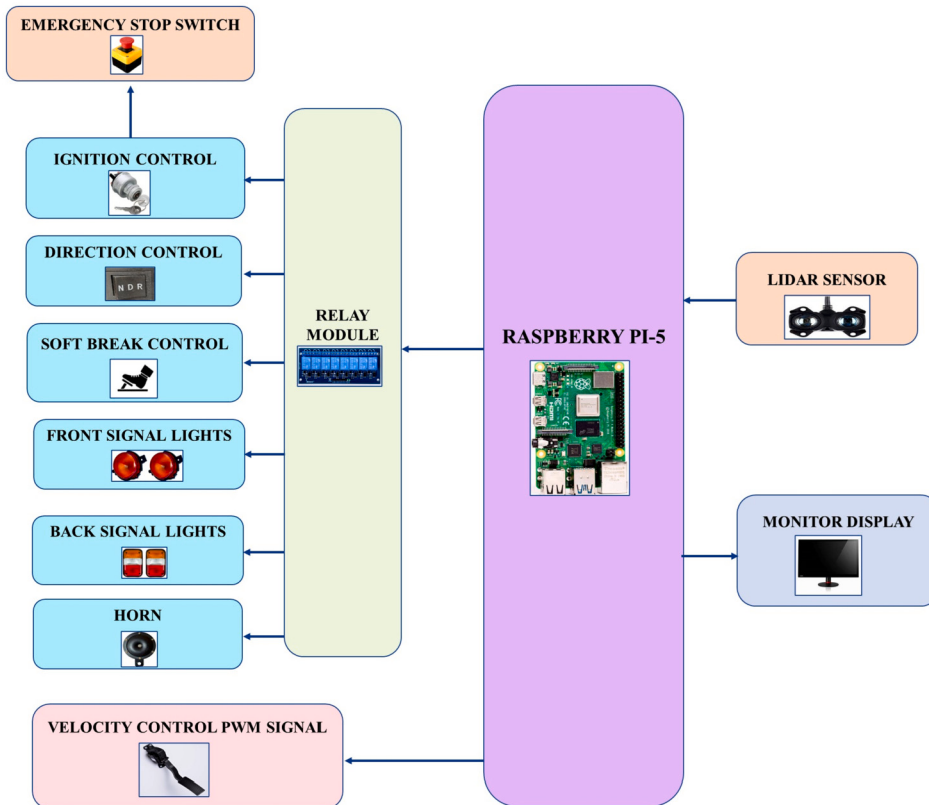


Fig. 9. Block Diagram of Motion Control Unit for the Proposed System.

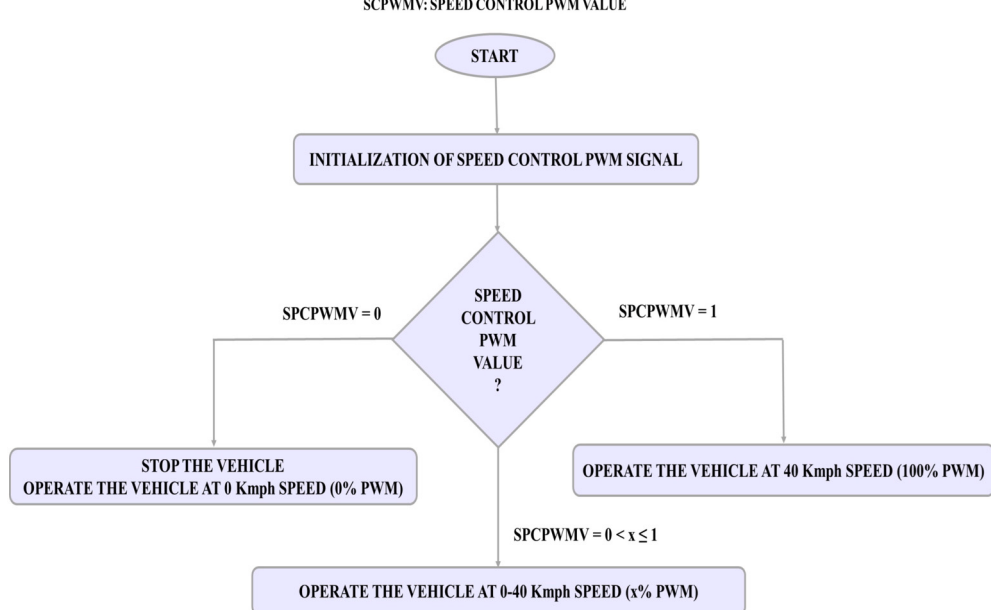


Fig. 10. Flow Chart of SPCPWM Signal.

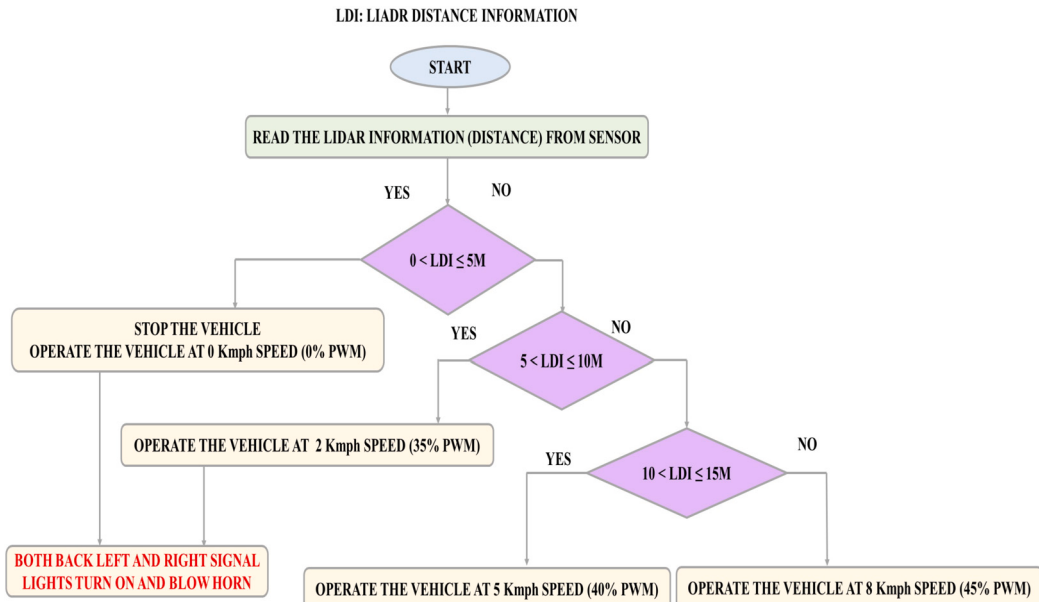


Fig. 11. Flow Chart of Integration of LIDAR and Motion Control Operation.

voltage progressively increases with the PWM duty cycle, starting from 0 V at 0% PWM and culminating at 2.8 V at 100% PWM. In contrast, at VAECUSP, the voltage across the speedometer remains at 0 V until the PWM duty cycle reaches 30%. Beyond this point, the voltage rises more sharply, attaining 24.5 V at 100% PWM. Furthermore, the speed remains at 0 Kmph until the PWM duty cycle reaches 35%, after which it escalates, reaching 40 Kmph at 100% PWM.

The connection diagram that interfacing of LIDAR sensor with raspberry pi is shown in Fig. 13 and the related connections are shown in Table 3.

In addition, the SoC sends control signals to an 8-channel relay module by using general purpose input output (GPIO) pins. The importance of relays in this setup lies in their ability to act as switches that can enable various automotive functions as shown in Table 4. The relay functions mainly focus on enabling the ignition, direction control, signal indications, blowing horn and braking, which are operating at differ-

**Table 3**  
LIDAR-Lite v3HP to Raspberry Pi 3 Pin Connections.

LIDAR-Lite v3HP Wire	Raspberry Pi 3 Pin
Blue	I2C SDA (Pin 3)
Green	I2C SCL (Pin 5)
Red	5 V Power (+)
Black	Ground (GND)

ent voltage levels. They isolate the low-voltage control signals from the Raspberry Pi from the higher-voltage circuits powering these functions. For instance, Relay 2 safely controls the high current required for ignition (around 60 V) by isolating the Raspberry Pi's low-voltage circuit. Meanwhile, relays 3, 4, 5, 6, 7 and 8 manage standard systems like turn signals, soft brake, and horn at 12 V without compromising safety.

**PWM: Pulse Width Modulation**  
**VARPP: Voltage Across Raspberry Pi PWM Pin**  
**VAECUSP: Voltage Across ECU Speedometer Pin**

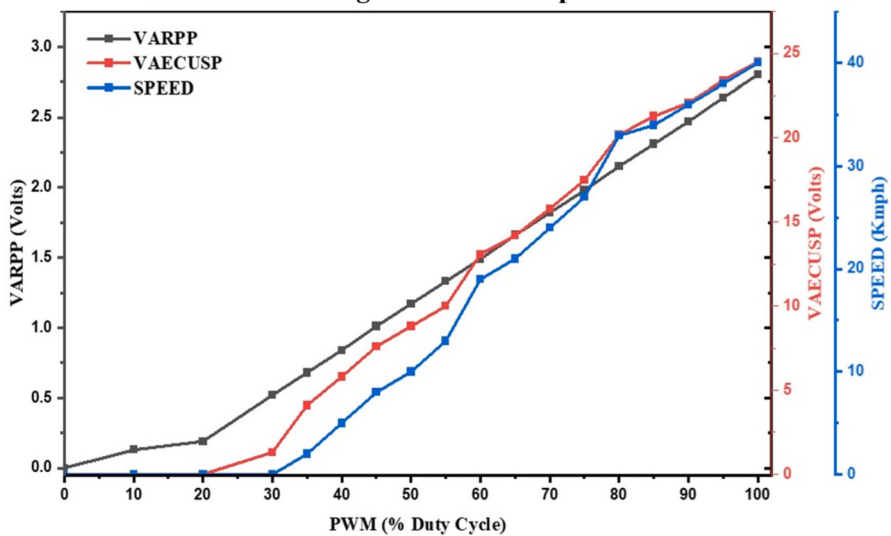


Fig. 12. PWM vs VARPP, VAECUSP and SPEED.

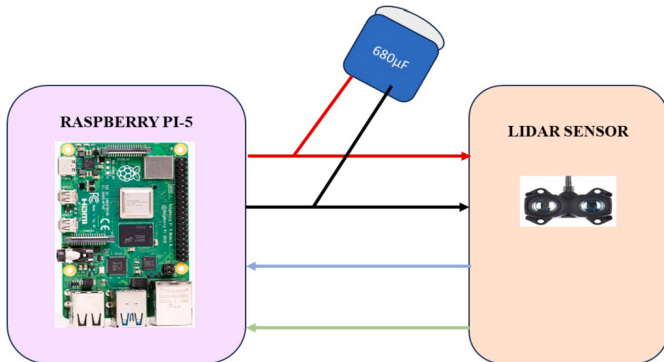


Fig. 13. Connection Diagram of Raspberry Pi 5 and LIDAR Sensor.

Table 4  
Control Actions.

Relay	Control actions	Description
Relay-1	Direction Control	Manages the vehicle's directional movements
Relay-2	Ignition Switch	Controls the power to start or stop the vehicle
Relay-3	Front Left Signal Light	Indicates a left turn at the front of the vehicle
Relay-4	Front Right Signal Light	Indicates a right turn at the front of the vehicle
Relay-5	Back Left Signal Light	Indicates a left turn at the rear of the vehicle
Relay-6	Back Right Signal Light	Indicates a right turn at the rear of the vehicle
Relay-7	Blow Horn	Generates a sound to alert others
Relay-8	Soft Break	Ensures smooth and gradual braking

Relay 1 precisely controls vehicle direction using the lower voltage typically 5 V. This capability is crucial for ensuring the safe and reliable operation of the vehicle's electrical components. The ignition control, operating at 60 V, relies on relay to manage the high voltage required to start the engine safely. The signals, soft brake and horn are functioning at 12 V. Additionally, direction control operates at 5 V. Real-time data and system status are displayed on a monitor to provide feedback to the user.

The working principle of a vehicle motion control shown in Fig. 14 outlines a control system using a single board computer, emergency stop switches, ignition switch, directional control, speed control and LIDAR sensor. Here it starts with an initialization and configuration of the GPIO

pins, LIDAR sensor and relay modules. Initially the vehicle is powered ON by activating the ignition relay switch (default in active) by using software command programmed on single board computer, this acts as the main power control that allows the system to proceed. If is OFF, the entire system remains shut down. After that the operator need to check the additional protection switches such as emergency stop switch status followed by steering control battery switch, this prioritizes safety. The emergency stop switch need to be set in the OFF position and steering control battery switch need to be set in the ON position to power up the vehicle in autonomous mode. After the completion of these checks, the AV-ECU is proceeding with the power-up sequence. Now, the selection of direction control of vehicle is chosen which provides input for the desired direction by activating or deactivating the direction control relay switch. By default, the relay switch is active that indicates the movement of vehicle in forward direction. Then speed of the vehicle is changed by using speed control PWM pin for desired speed based on the LIDAR data. The pin value ranges from 0 to 1 means 0 to 100% duty cycle. If the value is 0% duty cycle vehicle operating with 0 Km/h, indicates STOP the vehicle. If the value is 100% duty cycle the vehicle operating with maximum speed in our case nearly 40 Km/h. If the value is 'x', it may between 0 to 100% the speed of the vehicle varies between 0 to 40 Km/h. By default, the vehicle is operating at 45% duty cycle nearly 8 Km/h. Based on the condition, the work flow that was depicted in the Fig. 10 gives the motion controlling of vehicle.

The Fig. 15 shows the placement of signal lights, LIDAR sensor, EV-ECU and AV-ECU placements in the real time vehicle for motion control.

The Fig. 16 illustrates the implementation of motion control in response to obstacle detection. This system regulates the vehicle's speed based on data readings from the LIDAR sensor, which are displayed on the Raspberry Pi console.

### 3.2.2. Steering control

The process of achieving steering control in autonomous vehicles requires the precise manipulation of the vehicle's steering mechanism to accurately follow a specified path. This task involves an integrated system of sensors, actuators, and controllers working together seamlessly and which are responsible for accurately measuring the steering angle and determining the direction of rotation to ensure the vehicle operates smoothly and achieves precise control. The system's implementation overview of the working flow is illustrated in Fig. 17. This includes

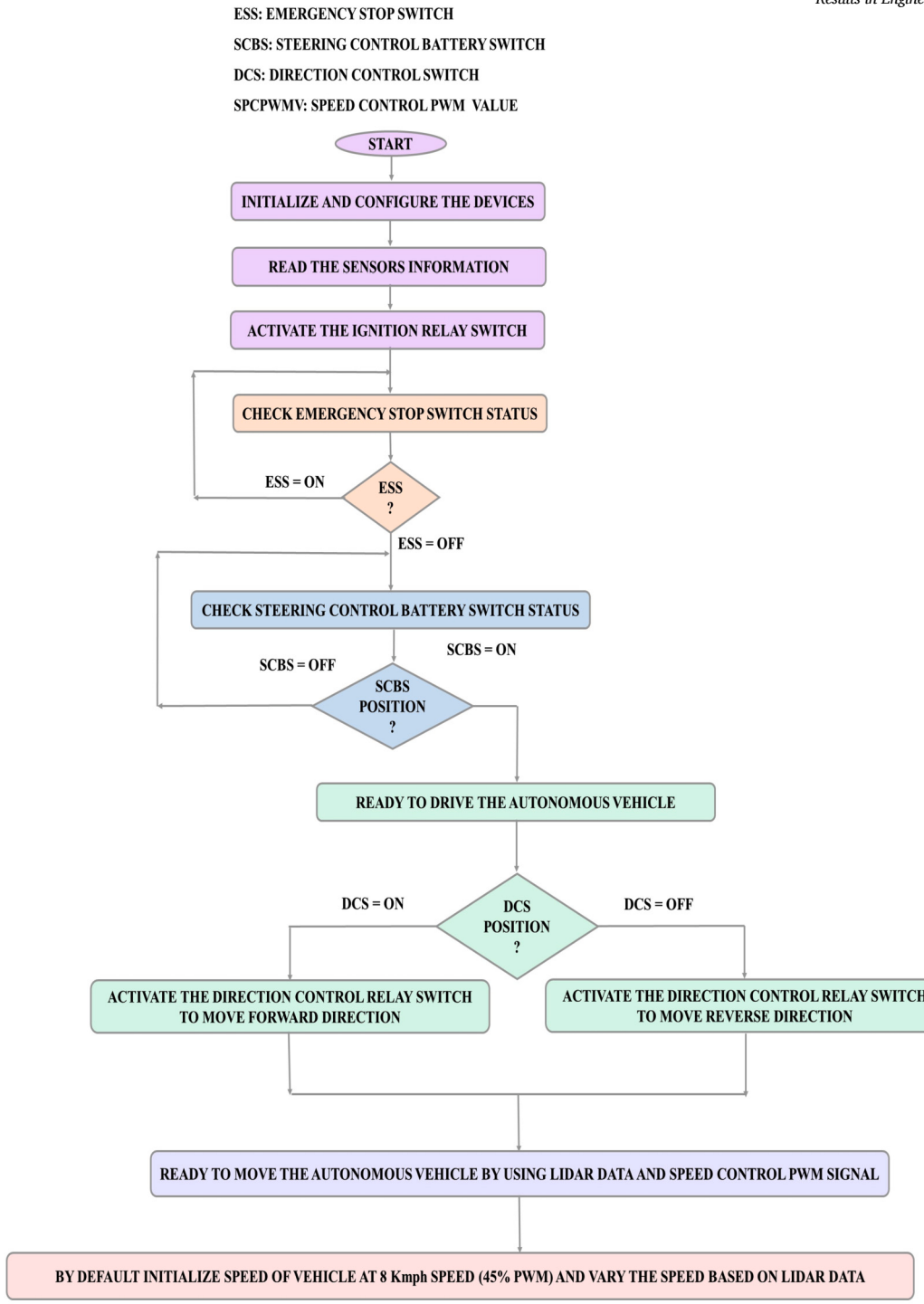


Fig. 14. Flow Chart of Vehicle Motion Control.

the initialization and configuration of components, as well as the control of the vehicle in various scenarios using sensors and actuators. The flowchart outlines the process for verifying sensor data and the status of key components, such as the steering control battery switch and the steering motor protection control signal, to initiate the control mechanism. Once these requisites are met, the system engages in steering control by utilizing information from the steering control pulse width modulation signal, motor driver direction pin, proximity sensor, and rotary encoder angle values.

The block diagram of this system illustrated in Fig. 18, shows how these components interact to control the steering mechanism. The sys-

tem is comprised of a raspberry pi serving as a single-board computer in the role of the controller, various sensors such as rotary and proximity sensors, and additional components such as a worm motor, motor driver, steering gears, and signal indicators. The integration of these components ensures precise and responsive steering control, adapting to different operational scenarios while maintaining safety and reliability.

To enable precise control over a significant load during autonomous steering, a worm gear motor was chosen for its high torque capabilities achieved through its internal mechanism. The chosen motor operates at 24 V DC, delivering  $\frac{1}{4}$  horsepower with a current draw of 7.8A and



Fig. 15. AV Signals, LIDAR, AV and EV-ECUs Placement.

```

File Edit Tabs Help
READING SENSORS INFORMATION
ACTIVATING IGNITION
PLEASE CHECK EMERGENCY STOP SWITCH CONDITION
PLEASE CHECK STEERING CONTROL BATTERY SWICH CONDITION
ACTIVATING DCS TO MOVE FORWARD
LIDAR DISTANCE MEASURED:
15
MOVING VEHICLE IN FORWARD DIRECITON WITH DEFAULT SPEED
LIDAR DISTANCE MEASURED:
8
SLOW DOWN THE VEHICLE
LIDAR DISTANCE MEASURED:
7
SLOW DOWN THE VEHICLE
LIDAR DISTANCE MEASURED:
4
STOP THE VEHICLE
LIDAR DISTANCE MEASURED:
3
STOP THE VEHICLE
```
Traceback (most recent call last):
  File "/home/zuber/motion.py", line 19, in <module>
    sleep(1)
KeyboardInterrupt
zuber@raspberrypi:~ $ 

```

Fig. 16. Visualization of Console Output for Motion Control.

a speed of 100 RPM (rotations per minute). To meet these operational requirements, a (Nearly 24 V) 26.7 V 15 mAh LiFePO<sub>4</sub> battery is used for providing sufficient power. To control the motor's direction (clockwise and anti-clockwise) and speed in terms of RPM, a Raspberry Pi controller interfaces with a motor driver. This driver is essential because Raspberry Pi pins cannot supply the high current required by the motor directly. A motor driver acts like an amplifier, taking the lower current control signal from the Raspberry Pi and using it to switch a much larger current flow from a separate power source to the motor.

For this purpose, the MD25HV H-Bridge motor driver depicted in Fig. 19 is employed, capable of handling motor voltages from 7 V to 58 V and currents up to 25A. The MD25HV motor driver enables bidirectional control of a worm motor, allowing clockwise (right) and anti-clockwise (left) rotations. Direction control is managed via the DIR pin through a program. The flowchart shown in Fig. 20 illustrates the two possible directions for controlling the steering motor. When the DIR pin signal is set to 0, the motor will rotate clockwise (to the right). Conversely, when the signal is set to 1, the motor will rotate counterclockwise (to the left).

After selecting the direction, motor speed in RPM is adjusted by varying the duty cycle of the PWM signal, as demonstrated in the flowchart outlined in Fig. 21. When SCPWM = 0, the motor receives no power, resulting in 0 RPM. SCPWM = 50 corresponds to a 50% duty cycle, yielding 50 RPM, while SCPWM = 100 maintains the motor at its full

**Table 5**  
Motor Driver Logic.

| DIR | PWM | MOTOR | Rotation Speed |
|-----|-----|-------|----------------|
| X   | 0   | BRAKE | 0 RPM          |
| 0   | 1   | RIGHT | 100 RPM        |
| 1   | 1   | LEFT  | 100 RPM        |

100 RPM speed. This integration of directional and RPM based speed control is efficiently managed by the motor driver.

The combined motor driver logic for both direction and steering control are outlined in Table 5. When the PWM signal is set to 0 V (0% duty cycle), regardless of the DIR value, the motor receives no power and the motor driver engages the brake mode, effectively stopping the motor. When DIR is set to 0 (logic low) and the PWM signal is set to 100% duty cycle, the motor driver sends continuous power to the motor, causing the motor to rotate clockwise to turn right the vehicle at full speed. Conversely, when DIR is set to 1 and the PWM signal is 1, the motor driver also sends continuous power to the motor, but in this configuration, the motor rotates in anticlockwise direction to turns left at full speed. The internal circuit operation for these scenarios involves the microcontroller generating the appropriate PWM signals and logic voltage levels for the DIR input, which the motor driver interprets to control the power delivery to the motor. If the PWM signal is set to a value between

**SCBS:** STEERING CONTROL BATTERY SWITCH  
**SMPCS:** STEERING MOTOR PROTECTION CONTROL SIGNAL  
**STC PWMV :**STEERING CONTROL PWM SIGNAL VALUE  
**MDDP:** MOTOR DRIVER DIRECTION PIN  
**PS:** PROXIMITY SENSORS 1 & 2  
**REA:** ROTARY ENCODER ANGLE

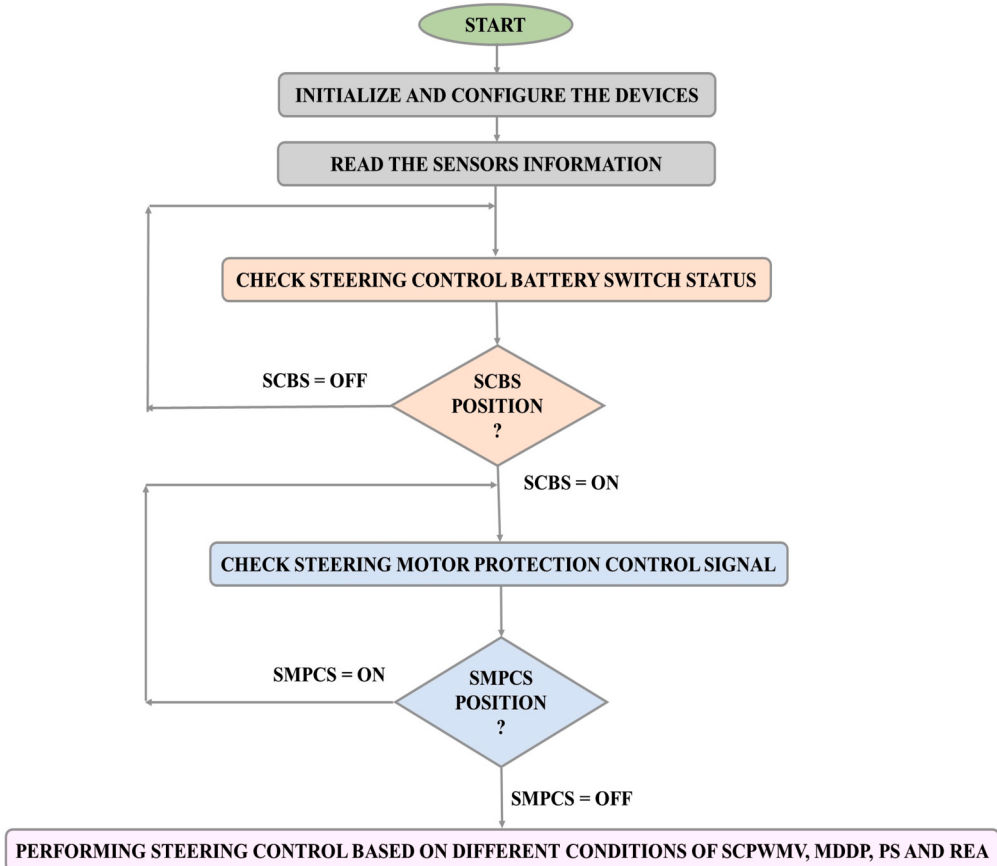


**Fig. 17.** Flow Chart of Autonomous Steering Control.

0 and 1 (between 0 to 100% duty cycle), the motor driver modulates the power accordingly, resulting in the motor running at an appropriate speed (0-100 RPM). The rotary encoder is crucial for precise steering control, providing real-time angular position and rotation direction data to the ECU. Table 5 outlines the four conditions based on the rotary encoder angle (REA):

- Condition 1 (DIR = X, PWM = 0, Motor = BRAKE, REA = Any Value):** The motor halts regardless of DIR or REA, ensuring the steering remains stationary. This state is typically protective, preventing unwanted motion.
- Condition 2 (DIR = 0, PWM = 1, Motor = RIGHT, REA ≤ 35):** The motor rotates clockwise to steer right while ensuring REA remains ≤ 35° for safe operation. If REA exceeds this limit, safety mechanisms like steering motor protection are activated.
- Condition 3 (DIR = 1, PWM = 1, Motor = LEFT, REA ≤ 35):** The motor rotates counterclockwise to steer left, with REA monitored to stay within safe limits, ensuring precise and controlled steering.
- Condition 4 (DIR = X, PWM = Any Value, Motor = STOP, REA > 35):** If REA exceeds 35°, the system halts the motor, activates the steering motor protection relay, and may disengage the ignition to prevent further movement, prioritizing safety.

In addition to the motor's rotation speed, precise control of the steering mechanism is crucial for the proper functioning of a vehicle's steering system [47]. This precise control is achieved through a gearing system comprising a driving gear mounted on the worm motor shaft and a driven gear connected to the steering system, as illustrated in Fig. 22.

Where, the driven gear, which has 38 teeth ( $N_1 = 38$ ), is larger and rotates more slowly but with greater torque. On the other hand, the driving gear, which has 15 teeth ( $N_2 = 15$ ), is smaller and rotates faster. A higher number of teeth on the driven gear relative to the driver gear means the driven gear will rotate more slowly. This is essential to achieve a specific gear ratio (GR) for applications requiring that reduces speed and increases torque in steering mechanism. The gear ratio is defined as the ratio of the number of teeth on the driven gear ( $N_1$ ) to the number of teeth on the driving gear ( $N_2$ ).

It can be calculated using equation (1):

$$GR = \frac{N_1}{N_2} = \frac{38}{15} \approx 1 : 2.53 \quad (1)$$

With a gear ratio of 2.53, the driven gear rotates 0.395 times for every single rotation of the driving gear. This gear ratio determines the reduction in speed when transferring power from the driving gear to the driven gear. Using this ratio, the speed of the driven gear can be calculated using equation (2) and is found to be 39.5 RPM.

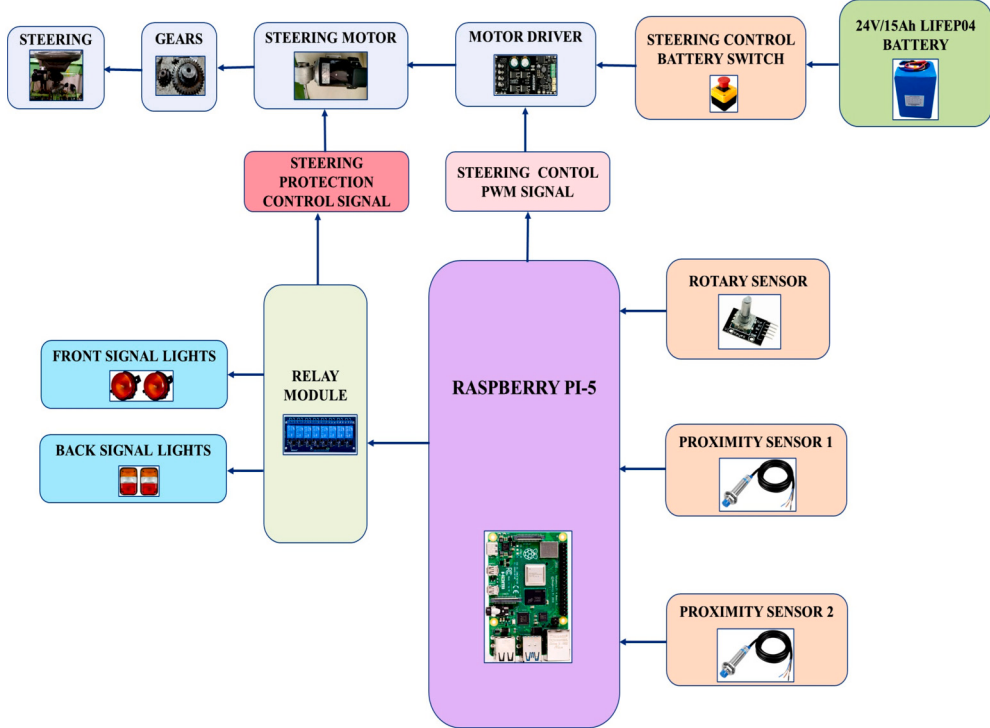


Fig. 18. Block Diagram of Proposed Automated Steering System.

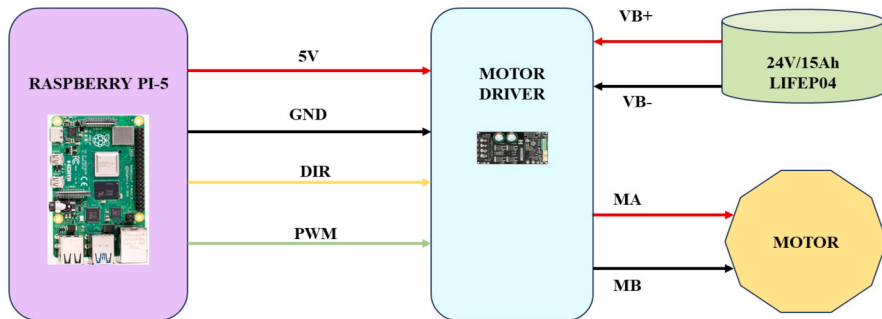


Fig. 19. Connection Diagram of Raspberry Pi 5 and Motor Driver.

MDDP: MOTOR DRIVER DIRECTION PIN

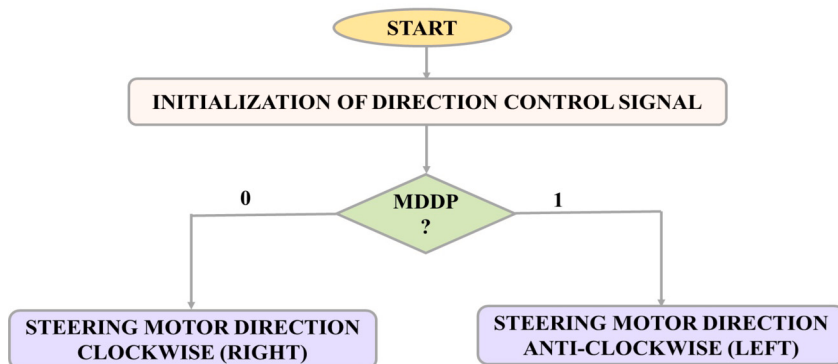


Fig. 20. Flow Chart of Direction Control Signal.

$$\text{Speed of drivengear} = \frac{\text{Motor Speed}}{\text{Gear Ratio}} = \frac{100 \text{ RPM}}{2.53} \approx 39.5 \text{ RPM} \quad (2)$$

The steering angle to wheel rotation ratio can be calculated by using a simple procedure by turning the steering wheel from lock to lock which means, turn the steering wheel fully to one side and count the total number of turns to the other side. According to this our vehicle has

a total no of steering wheel rotations 5 and wheel turns only 80 degrees.

Total angle of turn of front tyre wheel (W1) = 80 degrees

Total angle of rotation of steering wheel (W2) = Total no of steering wheel rotations \* 360 = 5 \* 360 = 1800 degrees

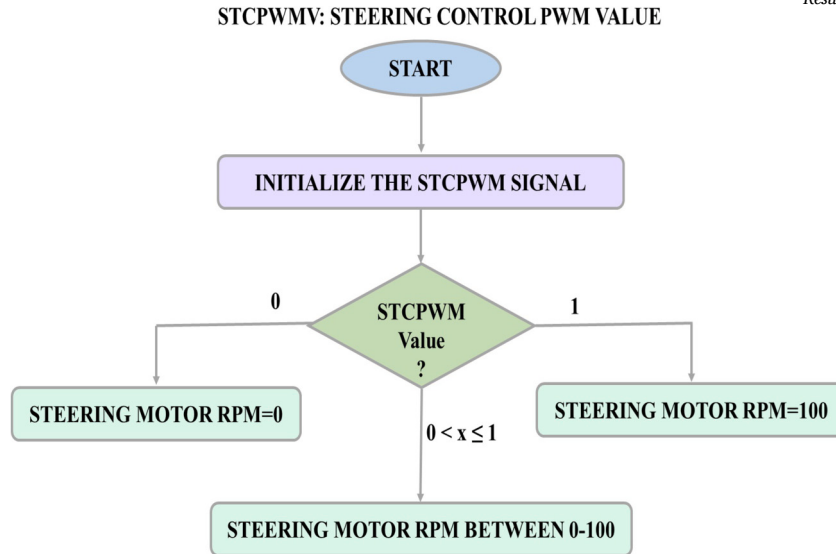


Fig. 21. Flow Chart of STCPWM Signal.



Fig. 22. Gears Mounted on Worm Motor and Steering Shafts.

The ratio is calculated in order to determine the extent to which or the angle to be rotated by the steering wheel when the wheel turns.

$$\text{Ratio} = \frac{W_1}{W_2} = \frac{80}{1800} = 1 : 22.5 \quad (3)$$

This mapping of the wheel to motor ratio is used to calculate the ratio between the wheel turn and the motor rotation. Since the motor is connected to the steering wheel via a gear drive, the gear drive ratio and the steering wheel ratio must be multiplied by the ratio between the wheel turn and the steering rotation.

From equations (1) and (3), The final ratio will determine the extent to which the motor needs to rotate for the vehicle wheel to turn by 1 degree.

$$\text{Ratio} = \frac{W_1}{W_2} * \frac{N_1}{N_2} = \frac{1}{22.5} * \frac{1}{2.53} = 1 : 56.925 \quad (4)$$

The graph shown in Fig. 23 illustrates how varying the PWM duty cycle affects different parameters in an electrical and mechanical system. By varying the PWM duty cycle, one can control the voltage delivered to a motor, the mechanical displacement of components, and the rotational speed of gears. The VARPP shows a linear increase in voltage across a PWM pin on the Raspberry Pi from 0 V at 0% PWM to 2.81 V at 100% PWM, indicating a direct proportional relationship between the PWM

duty cycle and the voltage. Similarly, the VAMDO reveals that the voltage across the motor driver output rises linearly from 0 V to 26.7 V as the PWM duty cycle increases, signifying that more power is delivered to the motor. The STRPS indicates mechanical displacement, with teeth shifts increasing from 0 at 0% PWM to 20.5 at 100% PWM, showing that the motor's mechanical output is directly influenced by the PWM duty cycle. Lastly, the DGRPS demonstrates that driving gear rotations per second grow from 0 to approximately 1.366667 as the PWM duty cycle increases to 100% PWM duty cycle.

#### Relate to Driven Gear and Wheel Rotation:

From the equation (4), the final ratio between the driving gear rotation and the wheel rotation was 1/56.925.

$$\text{DGRPS} = \frac{\text{STRPS}}{\text{Total No. of Teeth}} \quad (5)$$

$$\text{DGR Degrees Per Second (DGPDPs)} = \text{DGR Per Second} * 360 \quad (6)$$

$$\text{Wheel Rotation Angle Per Second (WRAPS)} = \text{DGRDPS} * \frac{1}{56.925} \quad (7)$$

The graph shown in Fig. 24 highlights the direct relationship between the PWM duty cycle and various rotational parameters in a mechanical system. By varying the PWM duty cycle, one can control the rotational speed and angular velocity of components such as gears and wheels. At 0% PWM, there is no rotational movement, indicated by all

**PWM: Pulse Width Modulation**  
**VARPP: Voltage Across Raspberry Pi PWM Pin**  
**VAMDO: Voltage Across Motor Driver Output**  
**STRPS: Shift of Teeth with Reference when PWM Signal Applied**  
**DGRPS: Driving Gear Rotations Per Second**

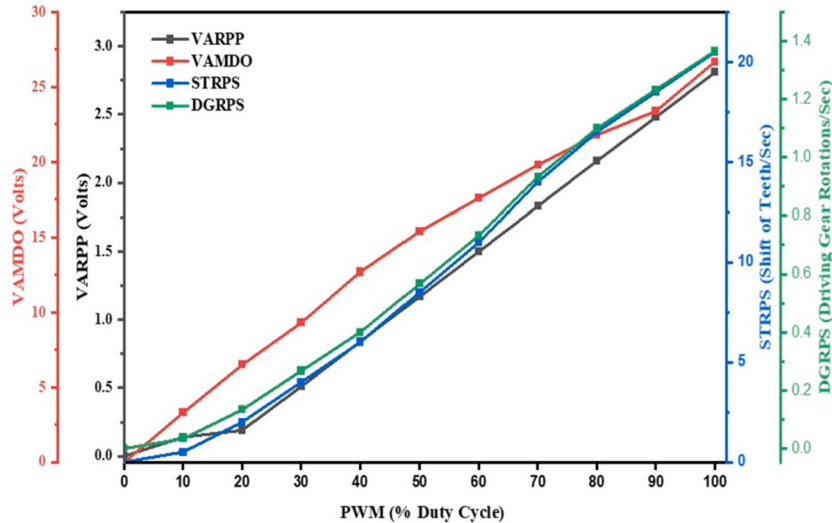


Fig. 23. PWM vs VARPP, VAMDO, STRPS and DGRPS.

**PWM: Pulse Width Modulation**  
**DGRPS: Driving Gear Rotations Per Second**  
**DGRDPS: Driving Gear Rotations Degrees Per Second**  
**WRAPS: Wheel Rotation Angle Per Second**

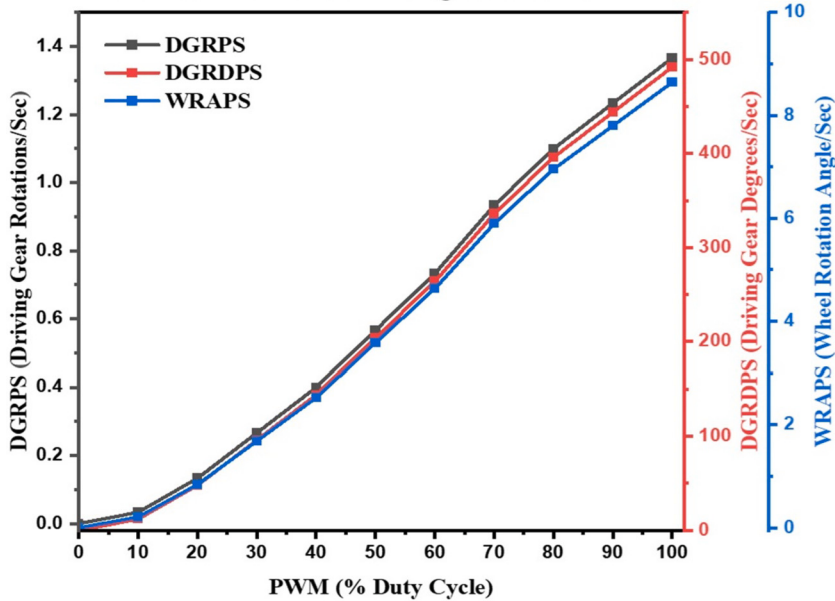


Fig. 24. PWM vs DGRPS, DGRDPS and WRAPS.

parameters being zero. As the PWM duty cycle increases, all parameters (DGRPS, DGRDPS, and WRAPS) increase linearly. For instance, at 50% PWM, the driving gear rotates at approximately 0.566667 rotations per second, with an angular velocity of 204 degrees per second, and the wheel rotates at 3.583662714 degrees per second. At 100% PWM, the driving gear rotation reaches 1.366667 rotations per second, with an angular velocity of 492 degrees per second, and the wheel rotation angle per second reaches 8.642951252 degrees.

The information presented in the graphs shown in Fig. 12, Fig. 23, and Fig. 24 will be utilized to adjust the vehicle's position to the left and right.

### 3.2.3. Soft left and right (to maintain straight path)

To move soft left and soft right, the PWM set to 20, the system produces a voltage of 0.19 V at the Raspberry Pi PWM pin and 6.5 V at the motor driver output. This configuration enables the motor to achieve a positional shift of 2 teeth from the reference point. The motor's driving

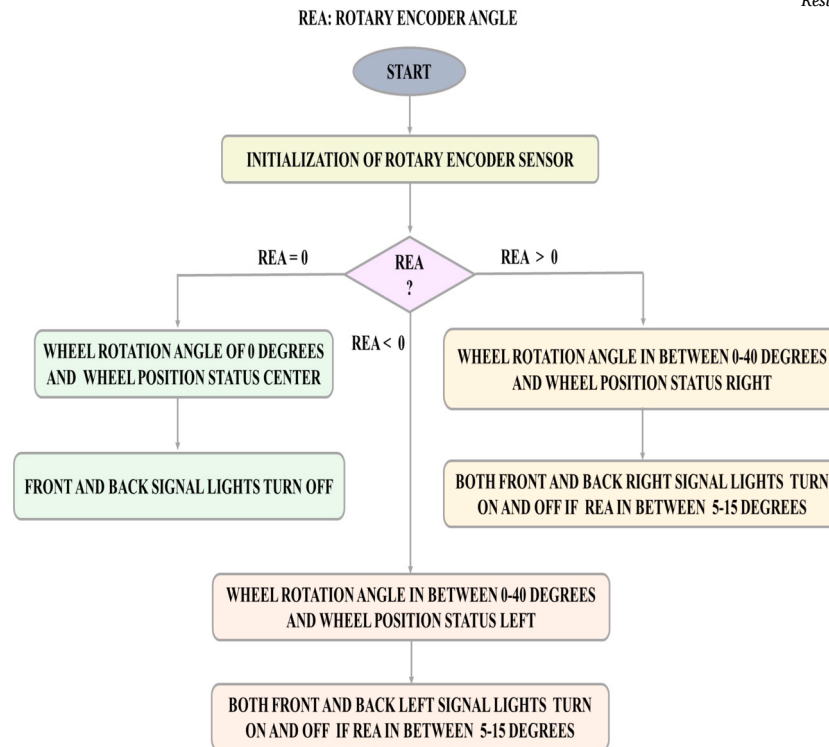


**Fig. 25.** Flow Chart of Rotary Encoder Operation.

gear operates at a rate of 0.13333 revolutions per second, equivalent to 48 degrees per second, which results in the wheel rotating at an angle of 0.84321 degrees per second. Over the span of one second, the cumulative wheel angle is 0.84321 degrees, during which the motor executes gentle left and right turns. This indicates that the PWM setting effectively regulates the motor's speed and direction, facilitating precise angular displacement of the wheel and ensuring controlled maneuvering of the system.

#### 3.2.4. Turn left and right (to overtake)

In addition to this to overtake the vehicle the condition is to keep a PWM setting of 40, the system generates a voltage of 0.84 V at the Raspberry Pi PWM pin and 12.7 V at the output of the motor driver, resulting in a displacement of six teeth from a reference point. The driving gear operates at a speed of 0.4 revolutions per second, which is equivalent to 144 degrees per second. Consequently, the wheel rotates at an angle of 2.53 degrees per second. Over a duration of five seconds, this results in a cumulative wheel angle of 12.65 degrees. The motor's performance indicates that a higher PWM setting leads to more substantial wheel movement, enabling a left or right turn with increased angular displacement and velocity compared to prior settings.

Furthermore, the steering wheel's turn angle in relation to the steering rotation is assessed using a rotary encoder sensor, commonly referred to as a shaft encoder. This sensor is positioned at the center of the driving gear, which is mounted on the worm motor shaft. The rotary encoder module comprises DT and CLK pins, and the determination of direction and rotational angle through encoders involves analyzing the phase relationship and frequency between these two signals. To identify the direction of rotation, these signals are phase-shifted by 90 degrees, allowing for the assessment of clockwise or counterclockwise movement based on their relative timing. The overall angle of rotation can be calculated by counting the number of pulses produced by the CLK signal. For more accurate angle measurement, an incremental encoder can be utilized, which generates a specific number of pulses per revolution. This sensor is adjusted to monitor the movement of the steering soft left and soft right to maintain straight path direction of the vehicle and also to

**Table 6**  
Motor Driver Logic.

| Conditions  | PS-1 | PS-2 | REA                        | SMP Switch | Ignition Switch |
|-------------|------|------|----------------------------|------------|-----------------|
| Condition-1 | 0    | 0    | $\leq 35$                  | OFF        | ON              |
| Condition-2 | 0    | 1    | $\leq 35 \text{ or } > 35$ | ON         | OFF             |
| Condition-3 | 1    | 0    | $\leq 35 \text{ or } > 35$ | ON         | OFF             |
| Condition-4 | 1    | 1    | $\leq 35 \text{ or } > 35$ | ON         | OFF             |

PS-1: Proximity Sensor-1, PS-2: Proximity Sensor-2.

SMP: Steering Motor Protection.

turn left and turn right in overtake conditions as discussed previously. Additionally it is used as one of the parameters for protecting steering motor.

The workflow presented in Fig. 25 is utilized to analyze the angle and direction of the wheel. If the  $REA = 0$ , the wheel turn angle is 0 degrees, indicating the straight position. If  $REA > 0$ , the wheel turn angle is between 0-40 degrees, indicating a RIGHT direction. If  $REA < 0$ , the wheel turn angle is between 0-40 degrees, indicating a LEFT direction. In addition to measuring angle and direction, the rotary encoder serves a crucial function in the protection of the steering motor by working in conjunction with proximity sensors placed near the front left and right wheels. The locations of the rotary encoder sensor and proximity sensors on the vehicle are depicted in Fig. 26. These sensors are designed to activate the steering protection relay when the REA exceeds 35 degrees in either direction as shown in Fig. 27 console output from raspberry pi. When this happens, the controller will instruct the steering protection control relay switch (Relay 9) to disconnect power to the steering motor to prevent any physical harm. Furthermore, the ignition switch (Relay 2) will be disabled simultaneously to bring the vehicle to a controlled stop. For additional details on the protection of the steering motor and ignition OFF operating conditions are presented in Table 6.

Fig. 28 illustrates the steering control system utilizing the AV-ECU, which is responsible for managing steering to maintain a straight path and facilitate vehicle overtaking without relying on LIDAR data.



Fig. 26. Rotary and Proximity Sensor Placement.

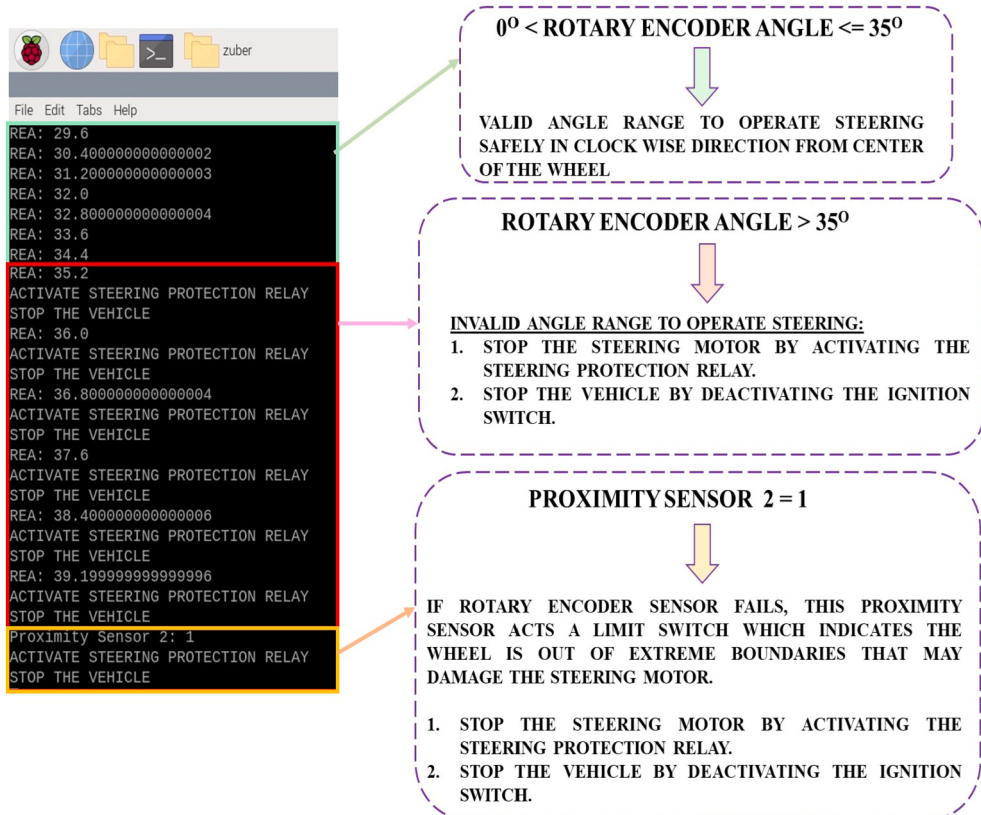


Fig. 27. Visualization of Console Output for Steering Protection Control.

### 3.3. Integration of essential systems in AEV

This section discusses the integration of EV-ECU with AV-ECU for the conversion of a standard EV to an AV with self-driving capabilities. The integration of EV control block, motion control block, steering control block represents the complete proposed block diagram illustrating the overall vehicle management, the vehicle ECU unit, and vehicle main dashboard front view are illustrated in Fig. 29, Fig. 30, and Fig. 31, respectively. The control flow of the AV transformation can be found in Fig. 32. The flowchart outlines the operational sequence of the autonomous vehicle, starting with system initialization which includes configuring devices and reading sensor data. Safety components such

as the emergency stop switch (ESS) and steering control battery switch (SCBS) are checked for proper functionality before activating the ignition relay to prepare the vehicle for autonomous operation. The vehicle determines the driving direction (forward or backward) based on input signals from the direction control, after verifying checks from LIDAR distance, proximity sensor values, and rotary encoder angle. The speed control and steering control are then set based on speed control PWM signal (SPCPWM) and the steering control PWM signal (STCPWM). The detailed descriptions provided in the flow diagram. The system determines the vehicle's speed and direction using LIDAR distance, proximity sensor readings, and calculated steering angle. An experimental setup was conducted to verify autonomous operation in an open space area

```

zuber@raspberrypi:~ $ python3 strctrl.PY
INITIALIZING AND CONFIGURING OF DEVICES
READING SENSORS INFORMATION
ACTIVATE IGNITION
PLEASE CHECK EMERGENCY STOP SWITCH CONDITION
PLEASE CHECK STEERING CONTROL BATTERY SWICH CONDITION
MOVE THE VEHICLE IN FORWARD DIRECTION
MOVING STEERING SOFTLY TO MOVE FORWARD STRAIGHT
SOFT RIGHT
SOFT LEFT
MOVING STEERING TO OVERTAKE
TURN RIGHT
TURN LEFT
MOVING STEERING SOFTLY TO MOVE FORWARD STRAIGHT
SOFT RIGHT
SOFT LEFT
MOVING STEERING TO OVERTAKE
TURN RIGHT
TURN LEFT
MOVING STEERING SOFTLY TO MOVE FORWARD STRAIGHT
SOFT RIGHT
SOFT LEFT

```

**MOVING STEERING SOFTLY TO MAINTAIN STRAIGHT FORWARD DIRECTION**

**MOVING STEERING TO OVERTAKE**

Fig. 28. Output Console of Operating Steering to Move Straight and Overtake.

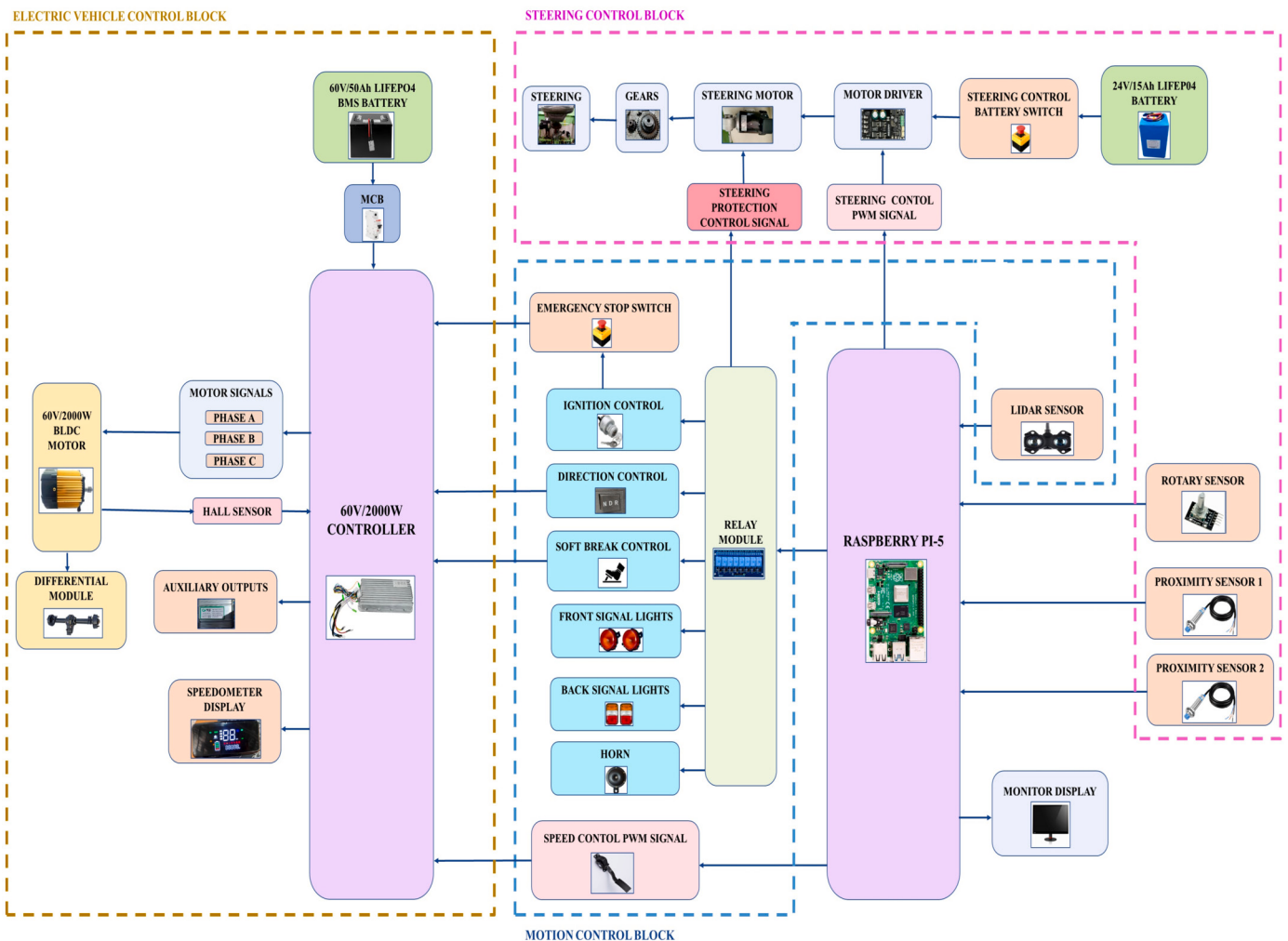


Fig. 29. The Proposed Combined Speed, Motion and Steering Control Block Diagram.

and conditions of straight road single direction traffic, considering only the direction control in the forward direction. Further verification is needed in traffic direction conditions as well as the reverse direction.

Fig. 33 demonstrates the motion and steering control system utilizing the AV-ECU, which is responsible for managing both the speed (default) and steering angle to ensure the vehicle maintains a straight trajectory

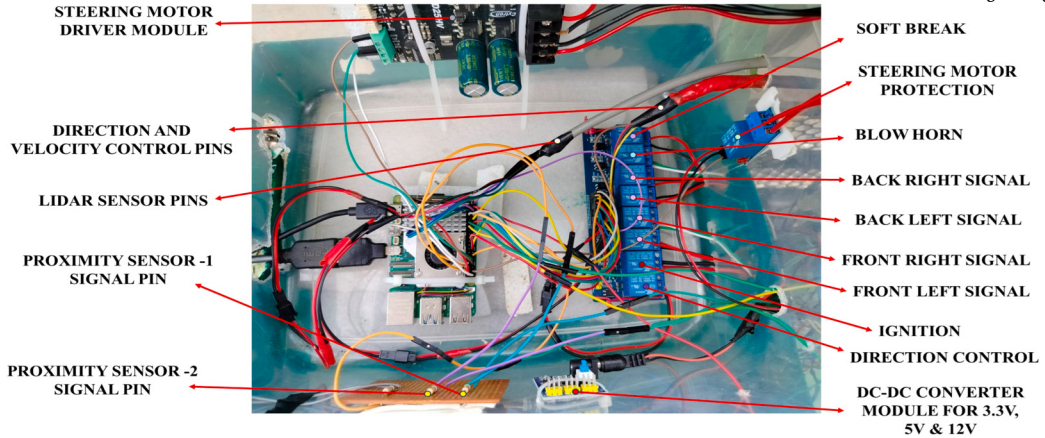


Fig. 30. Autonomous Vehicle ECU Part.

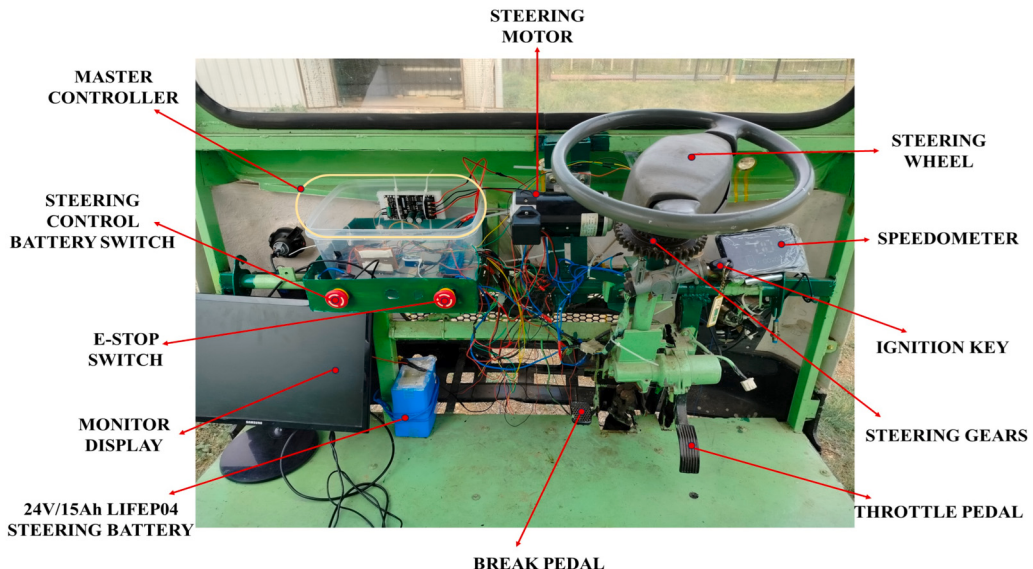


Fig. 31. Autonomous Vehicle Main Panel View.

(soft left and right adjustments) while proceeding forward based on LiDAR distance data.

Fig. 34 illustrates the motion and steering control system that employs the AV-ECU, which manages both speed and steering in accordance with LiDAR data. This figure highlights various conditions for moving the vehicle forward in a straight direction as well as for overtaking scenarios.

Additionally, to address the cost computation, excluding the main vehicle components (e.g., chassis, body, and primary vehicle construction), we have provided an analysis focusing exclusively on the additional components enabling autonomous and manual driving functionalities. The approximate costs include the slave controller (EV-ECU) at INR Rs.1,15,000, the master controller (AV-ECU) powered by a Raspberry Pi 5 at INR Rs.15,000, and other components such as the steering motor, sensors, control system modules, and relays totaling approximately INR Rs.55,000. This brings the overall cost of the additional components to approximately INR Rs.1,85,000, highlighting the system's cost-effectiveness compared to commercial autonomous vehicle solutions, which often exceed several lakhs for similar functionalities. The cost-effective design further underscores the feasibility and scalability of the proposed system for localized applications such as campus environments.

#### 4. Conclusion and future scope

This study successfully demonstrated the transformation of a conventional EV into a dual-mode AV designed for operation in a controlled campus environment. The system provides seamless transitions between manual and autonomous modes, showcasing its ability to balance traditional driving functionalities with automation. Key features such as LiDAR-based obstacle detection, PWM-based adaptive speed control, and a worm gear-driven steering mechanism ensure precise and reliable navigation. Safety measures, including emergency stop mechanisms and proximity sensor-based protection relays, further enhance the robustness of the system. Compared to existing works, it distinguishes itself by integrating a dual-mode control system and focusing on energy efficiency through regenerative braking in its practical implementation, scalability, and cost-effectiveness. Testing in a real-world environment validated the system's performance. The LiDAR sensor demonstrated accuracy up to 40 meters with  $\pm 2.5$  cm precision, dynamically adjusting the vehicle's speed according to object proximity. Steering was precise, with a 1:22.5 ratio and a 35° safety threshold, bolstered by fail-safe features like an emergency stop switch. Compared to existing works, this system emphasizes cost-effective implementation without compromising functionality, safety, or adaptability. Its dual-mode operation and focus on localized applications make it a scalable solution for smart

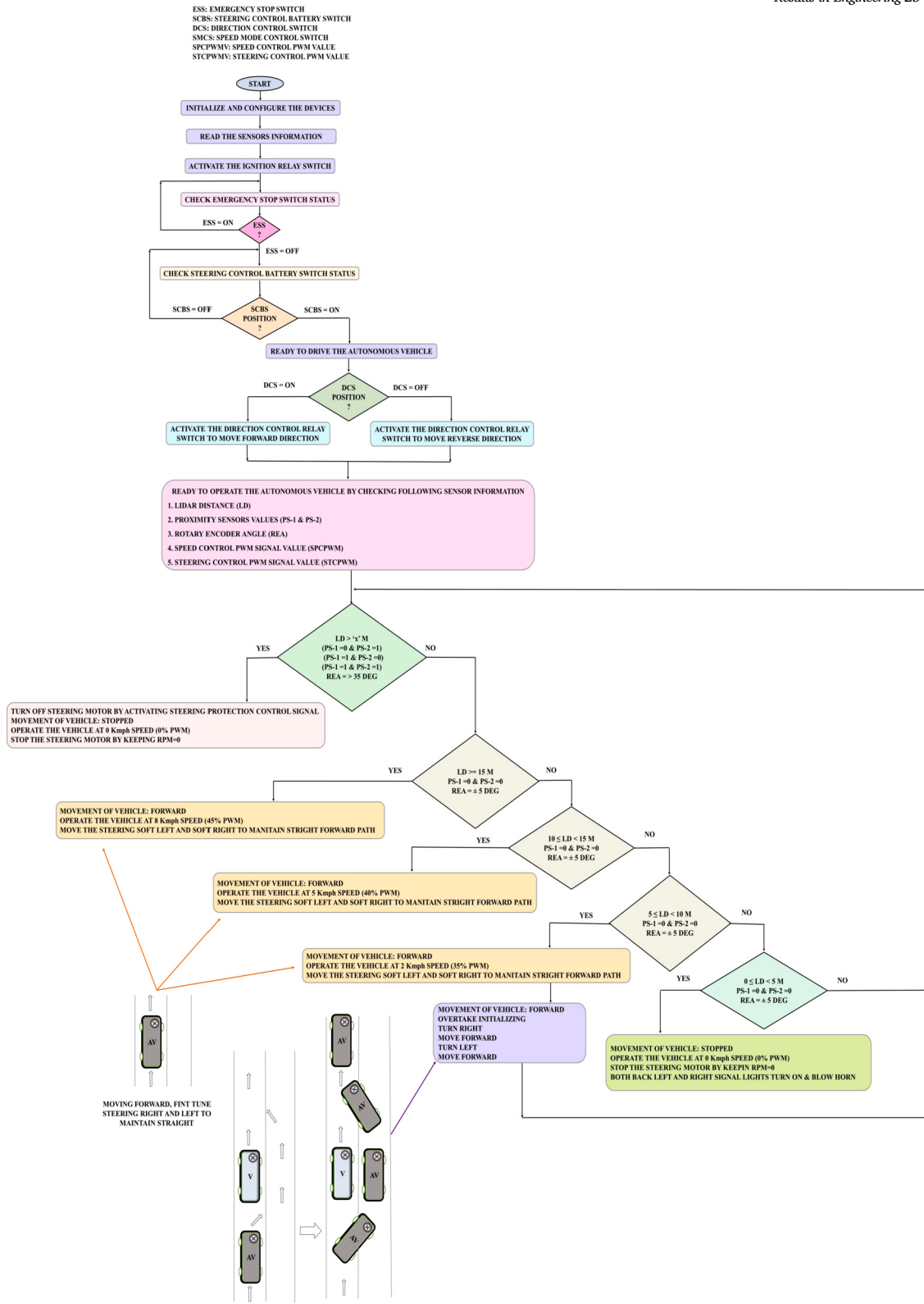


Fig. 32. Flow Chart of Proposed System.

campus transportation. Future developments include integrating additional sensors, advanced object detection algorithms, V2V and vehicle-to-infrastructure (V2I) communication protocols, and machine learning techniques to further enhance the system's capabilities for complex scenarios.

#### CRediT authorship contribution statement

**Zuber Basha Shaik:** Writing – review & editing, Writing – original draft, Visualization, Validation, Methodology, Investigation, Formal analysis, Data curation, Conceptualization. **Samineni Peddakrishna:**

```

zuber@raspberrypi:~ $ python3 main.py
INITIALIZING AND CONFIGURING OF DEVICES
READING SENSORS INFORMATION
ACTIVATE IGNITION
PLEASE CHECK EMERGENCY STOP SWITCH CONDITION
PLEASE CHECK STEERING CONTROL BATTERY SWICH CONDITION
ACTIVATING DCS TO MOVE FORWARD DIRECTION
LIDAR DISTANCE MEASURED: 25
MOVE FORWARD
SOFT RIGHT
SOFT LEFT
LIDAR DISTANCE MEASURED: 26
MOVE FORWARD
SOFT RIGHT
SOFT LEFT
LIDAR DISTANCE MEASURED: 25
MOVE FORWARD
SOFT RIGHT
SOFT LEFT
LIDAR DISTANCE MEASURED: 24
MOVE FORWARD
SOFT RIGHT
SOFT LEFT

```

Fig. 33. Visualization of Console Output when AV moving with No Obstacle Detected.

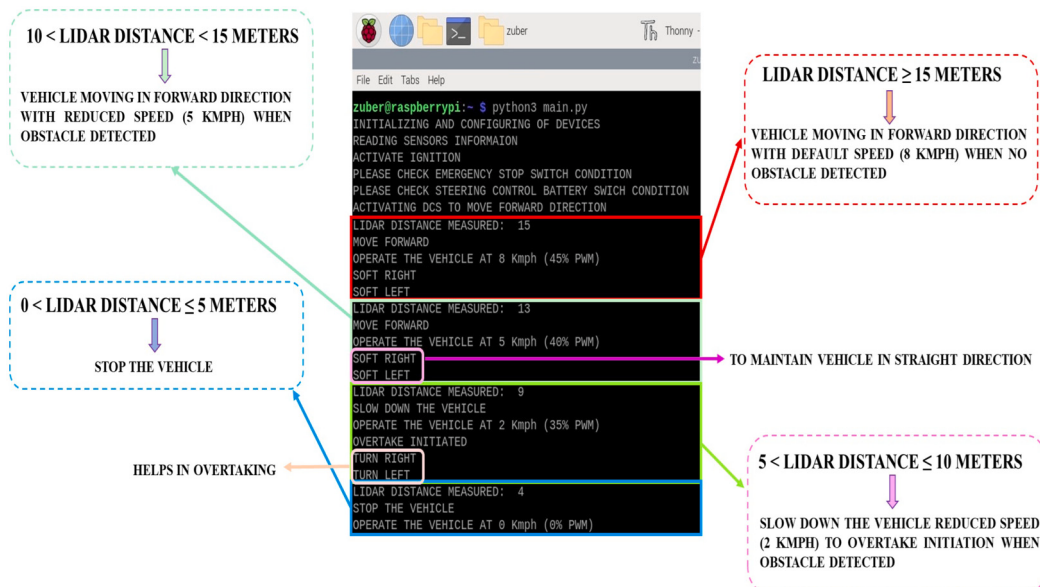


Fig. 34. Visualization of Console Output when AV moving with No Obstacle and Obstacle Detected.

Writing – review & editing, Writing – original draft, Visualization, Validation, Supervision, Software, Resources, Project administration, Methodology, Investigation, Funding acquisition, Formal analysis, Data curation, Conceptualization.

#### Disclaimer

The system presented in this manuscript is in the prototype phase and is intended solely for research and development purposes. Readers are advised to understand the limitations and experimental nature of the work.

#### Declaration of competing interest

The authors declare that they have no known competing financial interests or personal relationships that could have appeared to influence the work reported in this paper.

#### Acknowledgement

The authors would like to express their sincere gratitude to VIT-AP University for providing funding support through the specific grant under the RGEMS scheme (Project ID: RGEMS2021010). This work was completed under the RGEMS funding program.

#### Appendix A. Supplementary material

Supplementary material related to this article can be found online at <https://doi.org/10.1016/j.rineng.2025.103995>.

#### Data availability

No data was used for the research described in the article.

#### References

- [1] Sebastian Thrun, Mike Montemerlo, Hendrik Dahlkamp, David Stavens, Andrei Aron, James Diebel, Philip Fong, et al., Stanley: the robot that won the DARPA grand challenge, *J. Field Robot.* 23 (9) (2006) 661–692.
- [2] Chris Urmson, Joshua Anhalt, Drew Bagnell, Christopher Baker, Robert Bittner, M.N. Clark, John Dolan, Dave Duggins, Tugrul Galatali, Chris Geyer, et al., Autonomous driving in urban environments: boss and the urban challenge, *J. Field Robot.* 25 (8) (2008) 425–466.
- [3] Baidu Apollo, Baidu Apollo robotaxis, [Online]. Available, <https://apollo.auto>, 2023.
- [4] NAN, Model predictive control for autonomous vehicle path tracking through optimized kinematics, *Results Eng.* 24 (2024) 103123, <https://doi.org/10.1016/j.rineng.2024.103123>.
- [5] Rodolfo Orjuela, Jean-Philippe Lauffenburger, Jonathan Ledy, Michel Basset, Joel Lambert, Didier Bresch, Jean-Jacques Bockstaller, From a classic Renault Twizy to-

- wards a low cost autonomous car prototype: a proof of concept, IFAC-PapersOnLine 53 (2) (2020) 15161–15166.
- [6] Qasim Ajao, Oludamilare Olukotun, Safety challenges and analysis of autonomous electric vehicle development: insights from on-road testing and accident reports, arXiv preprint, arXiv:2305.12665, 2023.
- [7] R. Suganya, L.M.I. Leo Joseph, Sreedhar Kollem, Understanding lithium-ion battery management systems in electric vehicles: environmental and health impacts, comparative study, and future trends: a review, Results Eng. 24 (2024) 103047, <https://doi.org/10.1016/j.rineng.2024.103047>.
- [8] S. Rani, R. Jayaprakash, Review on electric mobility: trends, challenges and opportunities, Results Eng. 23 (2024) 102631, <https://doi.org/10.1016/j.rineng.2024.102631>.
- [9] James M. Anderson, Nidhi Kalra, Karlyn D. Stanley, Paul Sorenson, Constantine Samaras, Oluwatobi A. Oluwatola, Autonomous Vehicle Technology: A Guide for Policymakers, Rand Corporation, 2014.
- [10] Venkata Satya Rahul Kosuru, Ashwin Kavasseri Venkitaraman, Trends and challenges in electric vehicle motor drivelines-a review, Int. J. Electr. Comput. Eng. Syst. 14 (4) (2023) 485–495.
- [11] Ali Emadi, Handbook of Automotive Power Electronics and Motor Drives, CRC Press, 2017.
- [12] Mukhtar Oudeif, Saad Alshahrani, Hassan Abdallah, Autonomous vehicle sensors, in: Autonomous Vehicle Sensors, 2024.
- [13] Jun Tan, Lingfeng Wang, Integration of plug-in hybrid electric vehicles into residential distribution grid based on two-layer intelligent optimization, IEEE Trans. Smart Grid 5 (4) (2014) 1774–1784.
- [14] Jesús Balado, Ernesto Frías, Silvia M. González-Collazo, Lucía Díaz-Vilarinho, New trends in laser scanning for cultural heritage, in: New Technologies in Building and Construction: Towards Sustainable Development, Springer, 2022, pp. 167–186.
- [15] Jorge Martins, Francisco Brito, Carros eléctricos, Publindústria, Porto, Portugal, Dez, 2011.
- [16] Rogelio León, Christian Montaleza, José Luis Maldonado, Marcos Tostado-Véliz, Francisco Jurado, Hybrid electric vehicles: a review of existing configurations and thermodynamic cycles, Thermo 1 (2) (2021) 134–150.
- [17] Mehrdad Ehsani, Yimin Gao, Stefano Longo, Kambiz Ebrahimi, Modern Electric, Hybrid Electric, and Fuel Cell Vehicles, CRC Press, 2018.
- [18] Emmanuel Aramendia, Paul E. Brockway, Peter G. Taylor, Jonathan B. Norman, Matthew K. Heun, Zeke Marshall, Estimation of useful-stage energy returns on investment for fossil fuels and implications for renewable energy systems, Nat. Energy (2024) 1–14.
- [19] Jurgen Buekers, Mirja Van Holderbeke, Johan Bierkens, Luc Int Panis, Health and environmental benefits related to electric vehicle introduction in EU countries, Transp. Res., Part D, Transp. Environ. 33 (2014) 26–38.
- [20] Peter Weldon, Patrick Morrissey, Margaret O’Mahony, Long-term cost of ownership comparative analysis between electric vehicles and internal combustion engine vehicles, Sustain. Cities Soc. 39 (2018) 578–591.
- [21] Karl Georg Hoyer, The history of alternative fuels in transportation: the case of electric and hybrid cars, Util. Policy 16 (2) (2008) 63–71.
- [22] Steffen Bubeck, Jan Tomaschek, Ulrich Fahl, Perspectives of electric mobility: total cost of ownership of electric vehicles in Germany, Transp. Policy 50 (2016) 63–77.
- [23] Jia He, Hai Yang, Tie-Qiao Tang, Hai-Jun Huang, An optimal charging station location model with the consideration of electric vehicle’s driving range, Transp. Res., Part C, Emerg. Technol. 86 (2018) 641–654.
- [24] Suwaiba Mateen, Mohammad Amir, Ahteshamul Haque, Farhad Ilahi Bakhsh, Ultra-fast charging of electric vehicles: a review of power electronics converter, grid stability and optimal battery consideration in multi-energy systems, Sustain. Energy Grids Netw. (2023) 101112.
- [25] Björn Nykvist, Måns Nilsson, Rapidly falling costs of battery packs for electric vehicles, Nat. Clim. Change 5 (4) (2015) 329–332.
- [26] Darsh Parekh, Nishi Poddar, Aakash Rajpurkar, Manisha Chahal, Neeraj Kumar, Gyanendra Prasad Joshi, Woong Cho, A review on autonomous vehicles: progress, methods and challenges, Electronics 11 (14) (2022) 2162.
- [27] Yu Ming, Yanqiang Li, Zihui Zhang, Weiqi Yan, A survey of path planning algorithms for autonomous vehicles, SAE Int. J. Commer. Veh. 14 (02-14-01-0007) (2021) 97–109.
- [28] De Jong Yeong, Gustavo Velasco-Hernandez, John Barry, Joseph Walsh, Sensor and sensor fusion technology in autonomous vehicles: a review, Sensors 21 (6) (2021) 2140.
- [29] Karen Abrinia, Moosa Ayati, Hadi Niknam Shirvan, Amin Abazari, Ali Haddad Tabrizi, Mostafa Shahbazzadeh, Zeinab Maroufi, Mohammadreza Akrami, Erfan Safaei, Amirhossein Oliaei Fasakhoodi, et al., Advanced driving assistance system using distributed computation on single-board computers, in: 2019 7th International Conference on Robotics and Mechatronics (ICRoM), 2019, pp. 392–397.
- [30] Gurjashan Singh Pannu, Mohammad Dawud Ansari, Pritha Gupta, Design and implementation of autonomous car using Raspberry Pi, Int. J. Comput. Appl. 113 (9) (2015).
- [31] A. Mohammed, B. Ali, Low-cost autonomous car level 2: design and implementation for conventional vehicles, Results Eng. 17 (2023) 100969.
- [32] Ionut Alexandru Budisteanu, Using artificial intelligence to create a low cost self-driving car, in: Proc. 8th Int. Conf. Virtual Learn. (ICVL), 2013, pp. 1–7.
- [33] Nikhil Ollukaren, Kevin McFall, Low-cost platform for autonomous ground vehicle research, in: Proceedings of the 14th Early Career Technical Conference, vol. 13, No. 1, 2014.
- [34] R.W. Wall, J. Bennett, G. Eis, Creating a low-cost autonomous vehicle, in: IEEE 2002 28th Annual Conference of the Industrial Electronics Society (IECON 02), vol. 4, 2002, pp. 3112–3116.
- [35] Yueping Cui, Hao Xu, Jianqing Wu, Yuan Sun, Junxuan Zhao, Automatic vehicle tracking with roadside LiDAR data for the connected-vehicles system, IEEE Intell. Syst. 34 (3) (2019) 44–51.
- [36] Masaru Yoshioka, Naoki Suganuma, Keisuke Yoneda, Mohammad Aldibaja, Real-time object classification for autonomous vehicle using LiDAR, in: 2017 International Conference on Intelligent Informatics and Biomedical Sciences (ICIIIBMS), 2017, pp. 210–211.
- [37] T. Bécsi, Sz. Aradi, Á. Fehér, Gy. Gáldi, Autonomous vehicle function experiments with low-cost environment sensors, Transp. Res. Proc. 27 (2017) 333–340.
- [38] Jason Valera, Luigi Huaman, Lui Pasapera, Eduardo Prada, Luis Soto, Luis Agapito, Design of an autonomous electric single-seat vehicle based on environment recognition algorithms, in: 2019 IEEE Sciences and Humanities International Research Conference (SHIRCON), 2019, pp. 1–4.
- [39] Fadi T. El-Hassan, Experimenting with sensors of a low-cost prototype of an autonomous vehicle, IEEE Sens. J. 20 (21) (2020) 13131–13138.
- [40] M.M. Faisal, M.S. Mohammed, A.M. Abduljabar, S.H. Abdulhussain, B.M. Mahmood, W. Khan, A. Hussain, Object detection and distance measurement using AI, in: 2021 14th International Conference on Developments in eSystems Engineering (DeSE), 2021, pp. 559–565.
- [41] Ali Hakan Isik, Ömer Çetin, Multifunctional and low cost autonomous mobile robot, Gazi Mühendis. Bilim. Derg. 6 (2) (2020) 105–110.
- [42] P. Mariaraja, T. Manigandan, S. Arun, R.M. Meenakshi Sundaram, K. Dhenesh, Design and implementation of advanced automatic driving system using raspberry pi, in: 2020 5th International Conference on Communication and Electronics Systems (ICCES), 2020, pp. 1362–1367.
- [43] G. Lavanya, M. Deva Priya, A. Balamurugan, A. Christy Jeba Malar, An adaptive throttle and brake control system for automatic cruise control in disability support vehicle, in: Proceedings of the 4th International Conference on Smart City Applications, 2019, pp. 1–7.
- [44] Joko Slamet Saputro, M. Shafiy Widi Kresno Wibisono, Joko Hariyono, Miftahul Anwar, et al., Design of an adaptive cruise control system using PID control method on electric vehicle prototypes, in: 2023 International Conference on Advanced Mechatronics, Intelligent Manufacture and Industrial Automation (ICAMIMIA), 2023, pp. 599–605.
- [45] Ardhanra Putra Setyawan, Dedi Cahya Happyanto, et al., Implementation of intelligent speed control for autonomous electric vehicles, in: 2023 International Electronics Symposium (IES), 2023, pp. 58–63.
- [46] Sagar Shinde, Lalitkumar Wadhwa, Sheetalkumar Rawandale, Nitin Sherje, Shubham Jadhav, Ausmita Biswas, Kalyani Gupta, Advanced adaptive cruise control and vehicle to vehicle communication using LiDAR, Multidiscipl. Sci. J. 6 (2) (2024).
- [47] G. Amritthananda Babu, K. Guruvayoorappan, V.V. SajithVariyar, K.P. Soman, Design and fabrication of robotic systems: converting a conventional car to a driverless car, in: 2017 International Conference on Advances in Computing, Communications and Informatics (ICACCI), 2017, pp. 857–863.